

CHEMISTRY

A EUROPEAN JOURNAL

Supporting Information

© Copyright Wiley-VCH Verlag GmbH & Co. KGaA, 69451 Weinheim, 2013

Bispidine Platform Grants Full Control over Magnetic State of Ferrous Chelates in Water

Jacek Lukasz Kolanowski,^[a] Erwann Jeanneau,^[b] Robert Steinhoff,^[a] and Jens Hasserodt^{*[a]}

chem_201300604_sm_miscellaneous_information.pdf

Protocols and NMR spectra of ligands and intermediates	3
General Information	3
Piperidinone 1:	4
Intermediate 2:.....	4
L4:	7
L1:	9
3-Chloromethylpyridazine:.....	11
L2:	12
L3:	14
X-ray structural analyses of free ligands and ferrous complexes.....	16
Experimental	16
Figure S1 : L1 (CCDC 902550)	17
Figure S2 : FeL1 (CCDC 902554)	18
Figure S3 : FeL2 (CCDC 902552)	19
Figure S4 : FeL4(CH₃CN) (CCDC 902553)	20
Figure S5 : FeL4(SO₄) (CCDC 902296).....	21
Figure S6 : L3 (CCDC 902551)	22
Figure S7 : FeL3 (CCDC 904020)	23
NMR spectra and magnetic moments of complexes	24
Experimental	24
Thermodynamic parameters' estimation	24
FeL1 => spin transition	26
Figure S8: ¹ H NMR spectrum at in D ₂ O (298 K):.....	26
Figure S9: Comparison of FeL1 ¹ H NMR spectra at RT (298 K) in different solvents:	26
Figure S11 : Variable temperature ¹ H NMR spectra of FeL1 in CD ₃ CN (233 K - 333 K)	28
Figure S12 : Variable temperature ¹ H NMR spectra in Acetone-d6 (213 - 323 K)	29
Figure S13. Magnetic moments of FeL1 (Evans' method) at different temp.....	30
Figure S14. Nonlinear fitting curves of the spin transition of FeL1 in solution.....	31
FeL2 => low-spin	32
Figure S15: ¹ H NMR spectrum of FeL2 in D ₂ O (298 K):	32
Figure S16: Comparison of ¹ H NMR spectra of FeL2 at different temperatures (D ₂ O):.....	32
Figure S17: Magnetic moments of FeL2 (Evans' method) at different temperatures	33
FeL3 => low-spin	34
Figure S18: ¹ H NMR spectrum in D ₂ O	34
Figure S19: Temperature dependency (298 – 353 K) of ¹ H NMR spectra in D ₂ O.....	34
Figure S20: Magnetic moments of FeL3 (Evans' method) at different temperatures	35
FeL4(SO₄) => high spin.....	36
Figure S21 : ¹ H NMR spectrum of Fe4(SO ₄) in D ₂ O at 298 K (and zoom)	36
Figure S22: Magnetic moments of FeL4*SO ₄ (Evans' method) at different temperatures	36
Figure S23: Temperature variation of magnetic moment of FeL4*SO ₄ in the solid state (SQUID)	37
FeL4(CH₃CN) => ligand exchange leading to "intermediate" spin	38
Figure S24: ¹ H NMR spectra in CD ₃ CN (298 K)	38
Figure S25: Variable temperature ¹ H NMR spectra of FeL4*CH ₃ CN in CD ₃ CN (298 - 333 K)	38
Figure S26: Variable temperature ¹ H NMR spectra of FeL4*CH ₃ CN in Acetone-d6 (298 - 333 K)	39
Figure S27: Magnetic moments of FeL4*CH ₃ CN (Evans' method) at different temperatures	40
Cyclic voltammetry:	41
Figure S28. Cyclic voltammograms of FeL1, FeL2, FeL3 and [FeL4(CH ₃ CN)] in acetonitrile.....	41
References :	42

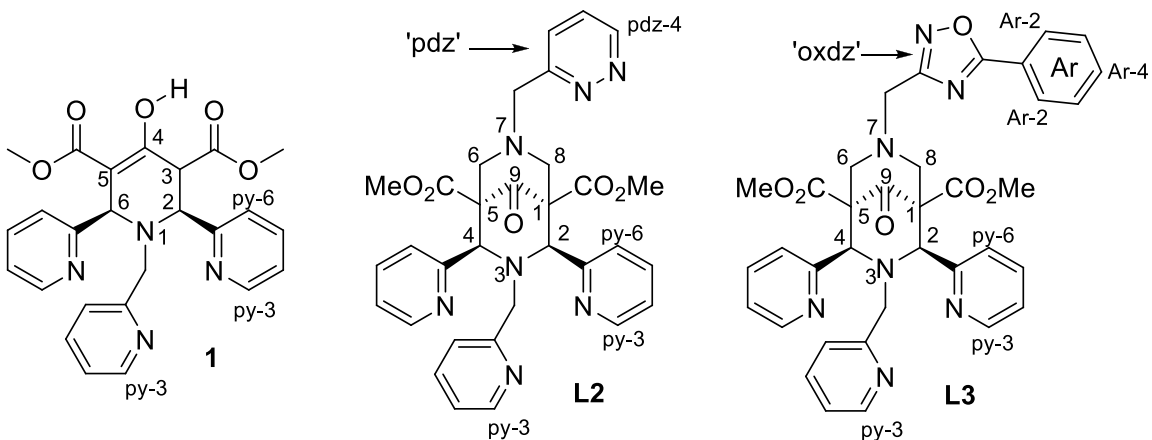
Protocols and NMR spectra of ligands and intermediates

General Information

Reagents and solvents were purchased from Aldrich, Acros and Alfa Aesar and used without further purification. Solvents were dried by standing the commercial dry HPLC grade solvents for 24 h on thermally-activated molecular sieves (3 Å for MeOH and EtOH, 4 Å for CH₃CN and Et₂O, sieve activation by 24 h heating at 315 °C) and degassed by a freeze-pump-thaw method (sequence repeated 3-5 times). Column chromatography was performed using Merck Aluminium oxide 90 active neutral (activity stage I, 0.063-0.200 mm mesh) or Merck silica gel Si-60 (40-63 µm). All NMR spectra were acquired on a Bruker DPX 200 (200.13 and 50.32 MHz for ¹H and ¹³C respectively) or on a Bruker AVANCE 500 (500.10 and 125.76 MHz for ¹H and ¹³C respectively) as indicated, at 298K (unless otherwise stated). Chemical shifts (δ) are reported in ppm (s = singlet, d = doublet, t = triplet, m = multiplet, br = broad) and referenced to solvent. NMR coupling constants (J) are reported in hertz. All signals in ¹H and ¹³C NMR spectra of organic molecules were unambiguously assigned and in order to do so, two-dimentional homo and/or heteronuclear NMR experiments were performed if necessary (COSY and/or NOESY/ROESY as well as HSQC and HMBC). Note the numbering for NMR signals (ESI below).

UV-vis spectra were recorded on V-670 Jasco spectrophotometer. High resolution mass spectrometry measurements and elemental analyses were performed at the “Centre Commun de Spectrometrie de Masse” of the University Claude Bernard in Lyon (France) and the Service Central d’Analyse of the CNRS in Solaize (France). Only crystalline batches of ferrous complexes of bispidines were used for analyses.

Usual numbering of ligands and precursors for NMR analysis:



Piperidinone 1:^[1] (2S,6R)-dimethyl 4-oxo-2,6-di(pyridin-2-yl)-1-(pyridin-2-ylmethyl)piperidine-3,5-dicarboxylate

To an ice-cold solution of acetone dicarboxylate (60.95 g; 350 mmol) in methanol (150 ml) was added dropwise picolyl aldehyde (82.54 g; 770 mmol) and picolyl amine (41.74 g; 385 mmol). The reaction was then stirred for 5 minutes on ice and then placed in the fridge overnight. The resulting white solid was washed with diethyl ether and recrystallised from ethanol. White, crystalline material formed was filtered off and washed with diethyl ether. The workup of the filtrates gave an additional material which was combined with the first crop yielding 132.30 g (82 %) of a pure product as white crystals. M.p. 130–133 °C; ¹H NMR (500 MHz, CDCl₃) δ_H 3.51 (3H, s, -CO₂CH₃), 3.75 (3H, s, -CO₂CH₃), 3.77 (2H, s, NCH₂py), 4.28 (1H, d, J=8.55, H-2), 4.78 (1H, d, J=9.40, H-3), 4.87 (1H, s, H-6), 7.10 (1H, dd, J=6.84, 5.13, pi H-4), 7.15 (1H, m, py H-4), 7.36 (2H, d, J=8.55, py H-6), 7.49 (1H, d, J=7.69, pi H-6), 7.55 (1H, td, J=7.69, 1.71, py H-4), 7.68 (3H, m, 2 x py H-3, 1 x pi H-5), 8.45 (2H, t, J=4.27, py H-3), 8.60 (1H, d, J=3.42, pi H-3), 12.56 (s, 1H, OH); ¹³C NMR (126 MHz, CDCl₃) δ_C 44.9 (C-5), 51.8 (CO₂CH₃), 52.7 (CO₂CH₃), 53.9 (NCH₂py), 59.8 (C-2), 61.8 (C-6), 98.2 (C-3), 122.2, 122.2, 122.6, 122.7, 122.9, 123.3 (py, pi C-3 + C-5), 136.4, 136.5, 136.8 (py, pi C-4), 148.6, 149.1, 149.2 (py, pi C-6), 158.3, 159.9, 161.5 (py, pi C-2), 167.7 (C-4), 171.5 (CO₂Me), 172.2 (CO₂Me).

Intermediate 2: (2R,4S)-dimethyl 7-(2,4-dimethoxybenzyl)-9-oxo-2,4-di(pyridin-2-yl)-3-(pyridin-2-ylmethyl)-3,7-diazabicyclo[3.3.1]nonane-1,5-dicarboxylate

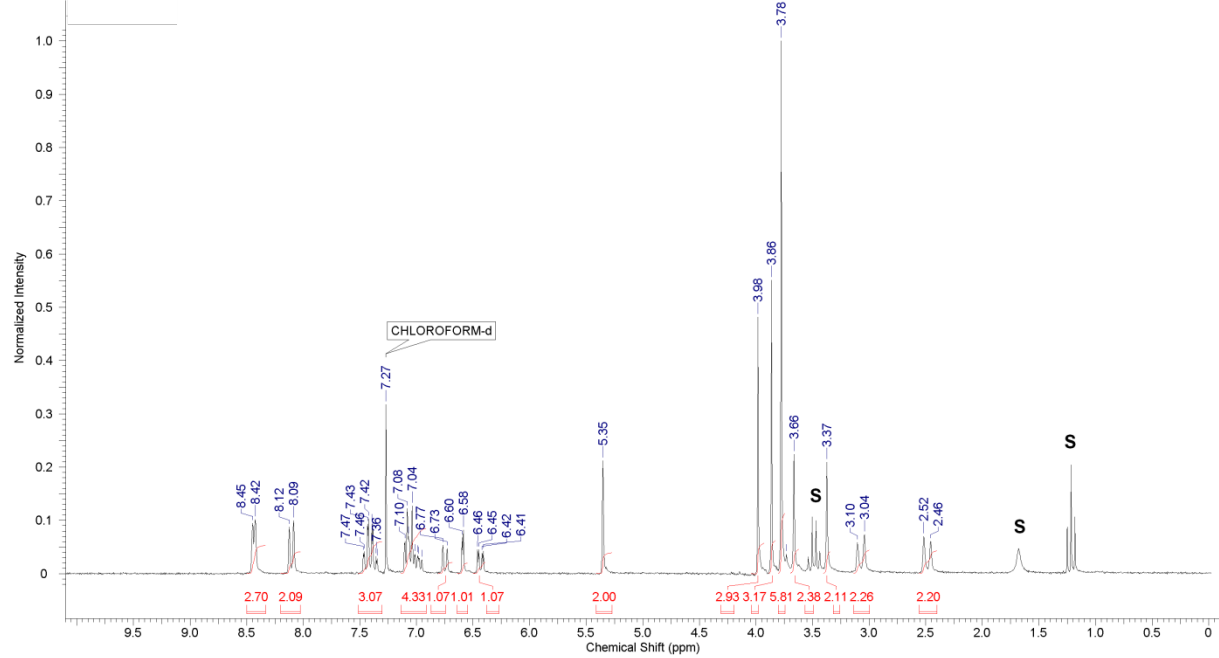
To a solution of piperidinone 1 (43.10 g; 93.6 mmol) in ethanol (600 ml), formaldehyde (37% in H₂O) (17.47 g, 215.3 mmol; 2.3 eq) and dimethoxybenzyl amine (18.00 g; 107.6 mmol; 1.15 eq) were added at 60°C. Then reaction mixture was stirred under reflux for 8h and all volatiles were removed under reduced pressure. The residue was dissolved on heating in a minimal quantity of methanol (50 ml) and to it diethyl ether was added (150 ml). White crystalline solid, which appeared after several hours at room temperature was filtered off and washed three times with diethyl ether. Working up of the resulting filtrate yields additional material which was combined with the first crop giving in total 12.89 g (21%) of a pure product. M.p. 187–190 °C; ¹H NMR (500 MHz, CDCl₃): δ=2.49 (2H, d, J=11.6, H-6/8 eq.), 3.07 (2H, d, J=11.9, H-6/8 ax.), 3.37 (2H, s, N7-CH₂Ar), 3.66 (2H, s, N3-CH₂py), 3.78 (6H, s, -CO₂CH₃), 3.86 (3H, s, Ar4-OCH₃), 3.98 (3H, s, Ar2-OCH₃), 5.35 (2H, s, H-2/4), 6.43 (1H, dd, J=8.12, 2.14 Hz, CH₂Ar-5), 6.59 (1H, d, J=2.14 Hz, CH₂Ar-3), 6.74 (1H, d, J=7.69 Hz, N3-CH₂py-6), 6.97 (1H, ddd, J=7.59, 4.81, 0.85, N3-CH₂py-4), 7.01 - 7.16 (3H, m, CH₂Ar-4, CH₂Ar-6), 7.37 (1H, td, J=7.7, 1.7, N3-CH₂py-5), 7.42 (2H, td, J=7.7, 1.7, CH₂Ar-5), 8.10 (2H, d, J=8.12 Hz, CH₂Ar-6) 8.40 - 8.51 (3H, m, py, N3-CH₂py-3); jmod ¹³C NMR (126 MHz, CDCl₃): δ=52.5 (-CO₂CH₃), 55.5 (ArOCH₃), 55.5 (ArOCH₃), 55.8 (N3-CH₂py), 58.0 (N7-CH₂Ar), 59.4 (C-6/8), 62.2 (C-2/4), 70.6 (C-1/5), 98.7 (CH₂Ar-3), 103.8 (CH₂Ar-5), 117.6 (CH₂Ar-1), 121.6 (N3-CH₂py-4), 122.6 (CH₂Ar-4), 124.2 (N3-CH₂py-6), 124.7 (CH₂Ar-6), 133.1 (CH₂Ar-6), 135.5 (N3-CH₂py-5), 135.6 (CH₂Ar-5), 148.8 (CH₂Ar-4), 149.3 (N3-CH₂py-3), 156.4 (N3-CH₂py-1), 158.5 (CH₂Ar-2), 159.2 (CH₂Ar-4), 160.7 (CH₂Ar-1), 168.8 (CO₂CH₃), 204.1 (C-9). IR (solution in DCM) ν_{max}= 3051–2835 (C-H), 1738 (C=O), 1612 (Ar), 1589 (Ar), 1510 (Ar) cm⁻¹; HRMS (ESI): m/z calcd for C₃₆H₃₈N₅O₇: 652.2766 [M+H⁺]; found 652.2768; elemental analysis calcd (%) for C₃₆H₃₈N₅O₇: C 66.35, H 5.72, N 10.75; found: C 65.72, H 6.01, N 10.38.

NMR of *trans* isomer 2':

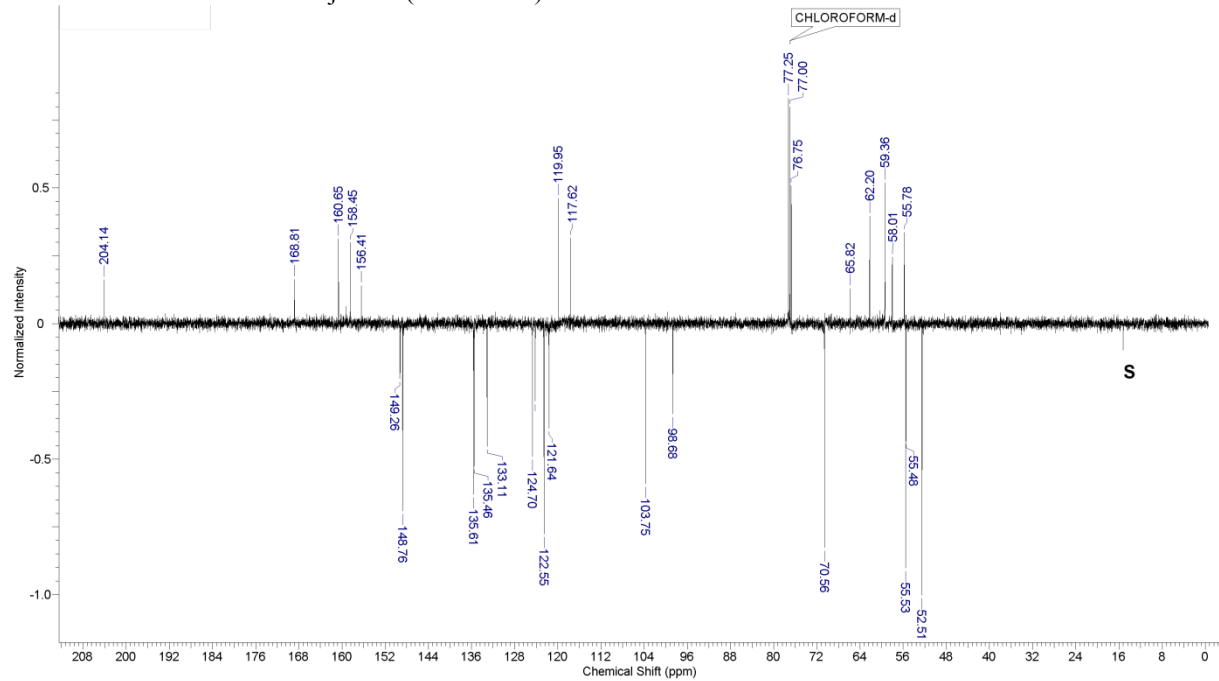
¹H NMR (500 MHz, CDCl₃) δ_H 2.81 (1 H, d, J=11.91 Hz, H-6 eq) 3.07 (1 H, d, J=11.00 Hz, H-8 eq) 3.40 (3 H, d, J=11.91 Hz, H-6 ax, N7-CH₂Ar, N3-CH₂py) 3.44 (3 H, s, C1-CO₂CH₃) 3.57 (1 H, d, J=11.00 Hz, N7-CH₂Ar) 3.64 (1 H, d, J=15.58, N3-CH₂py) 3.68 (1 H, d, J=11.00, H-8 ax) 3.79 (3 H, s, Ar4-OCH₃) 3.86 (3 H, s, C5-CO₂CH₃) 3.87 (3 H, s, Ar2-OCH₃) 4.87 (1 H, br. s., H-2 eq) 5.32 (1 H, s, H-4 ax) 6.44 (1 H, d, J=8.25 Hz, CH₂Ar-5) 6.53 (1 H, br. s., CH₂Ar-3) 6.95 - 7.09 (2 H, m, CH₂Ar-4, CH₂Ar-6) 7.09 - 7.20 (3 H, m, CH₂Ar-4 and py(ax)-6, N3-CH₂py-4) 7.43 - 7.52 (1 H, m, CH₂Ar-5) 7.52 - 7.59 (1 H, m, N3-CH₂py-5) 7.63 (1 H, t, J=7.79 Hz, CH₂Ar-6) 7.82 (1 H, d, J=7.33 Hz, N3-CH₂py-6) 8.09 (1 H, br. s., CH₂Ar-3) 8.36 (1 H, d, J=4.58 Hz, CH₂Ar-4) 8.50 (1 H, d, J=4.58 Hz, N3-CH₂py-3) 8.58 (1 H, d, J=4.58 Hz, CH₂Ar-5); ¹³C NMR – dept (126 MHz, CDCl₃) δ_C 51.92 (1 C, s, C1-CO₂CH₃) 52.45 (1 C, s, C5-CO₂CH₃) 55.14 (1 C, s, N3-CH₂py) 55.25 (1 C, s, Ar4-OCH₃) 55.35 (1 C, s, Ar2-OCH₃) 55.41 (1 C, s, N7-CH₂Ar) 60.51 (1 C, s, N7-CH₂Ar) 61.66 (1 C, s, C-COOMe C-1) 62.23 (1 C, s, C-COOMe C-5) 64.03 (1 C, s, N7-CH₂Ar) 67.22 (1 C, s, CH C-2) 68.78 (1 C, s, CH C-4) 98.55 (1 C, s, N7-CH₂Ar-3)

103.74 (1 C, s, Ar5) 117.55 (1 C, s, CH₂Ar-1) 121.73 (1 C, s, CH_{py}(ax)-4) 121.80 (1 C, s, N3-CH₂py-4) 122.36 (1 C, s, CH_{py}(eq)-4) 122.40 (1 C, s, N3-CH₂py-6) 122.93 (1 C, s, CH_{py}(ax)-6) 132.43 (1 C, s, CH_{py}(eq)-6) 135.91 (1 C, s, CH_{py}(eq)-5) 135.94 (1 C, s, CH_{py}(ax)-5) 136.77 (1 C, s, N3-CH₂py-5) 148.16 (1 C, s, CH_{py}(ax)-3) 148.70 (1 C, s, N3-CH₂py-3) 149.11 (1 C, s, CH_{py}(eq)-3) 156.11-156.17 (1 C, br.s., CH_{py}(ax)-1) 158.51 (1 C, s, CH_{py}(eq)-3) 158.88 (1 C, s, CH₂Ar-2) 159.44 (1 C, s, N3-CH₂py-1) 160.38 (1 C, s, CH₂Ar-2) 169.44 (1 C, s, COOMe) 169.96 (1 C, s, COOMe).

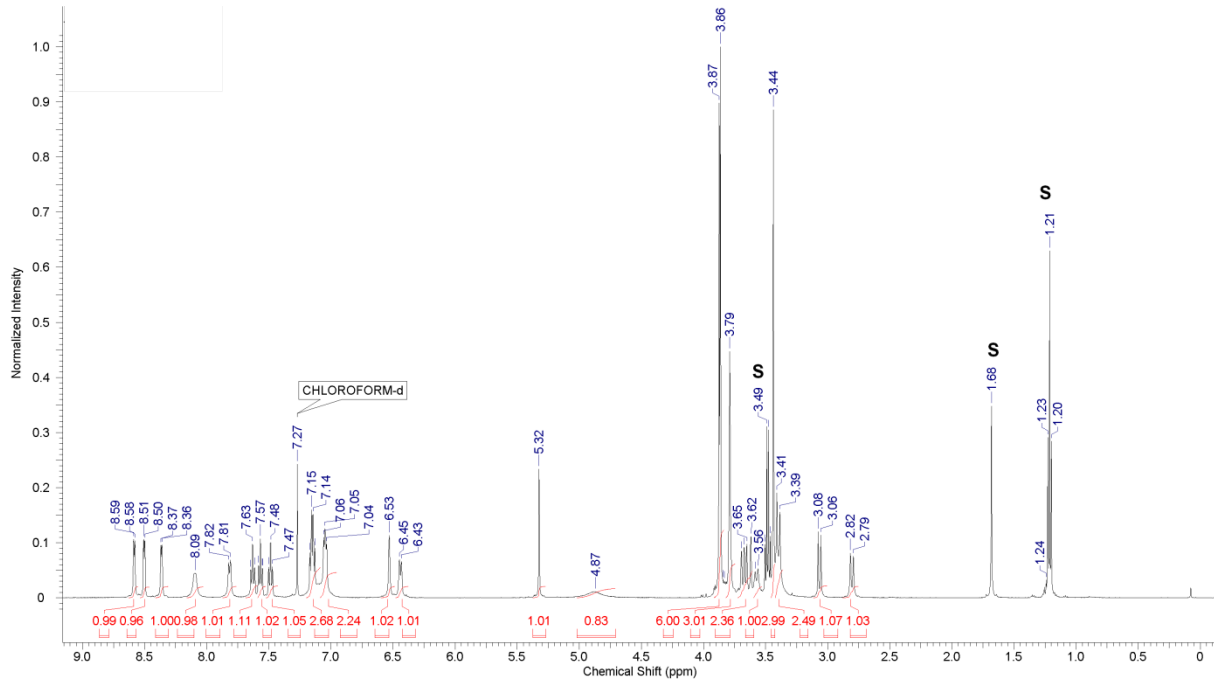
¹H NMR of *cis* isomer of **2**: (S = solvent)



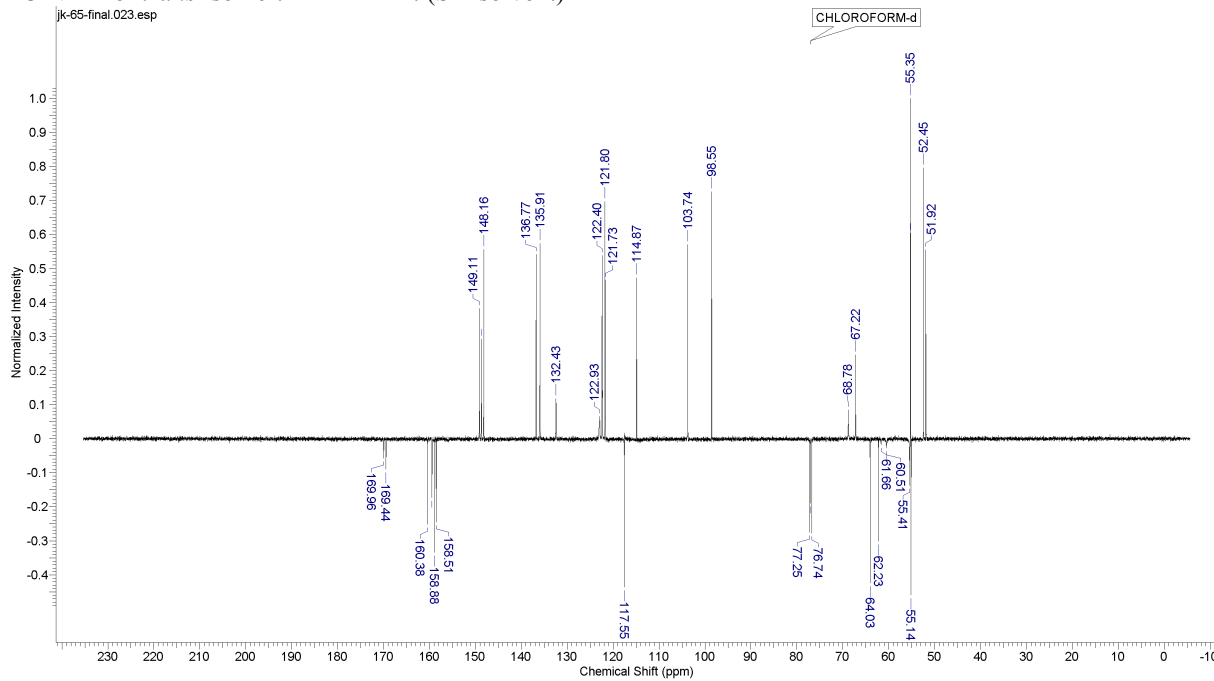
¹³C NMR of *cis* isomer of **2** – jmod : (S = solvent)



¹H NMR of *trans* isomer: **2'**: (S = solvent)

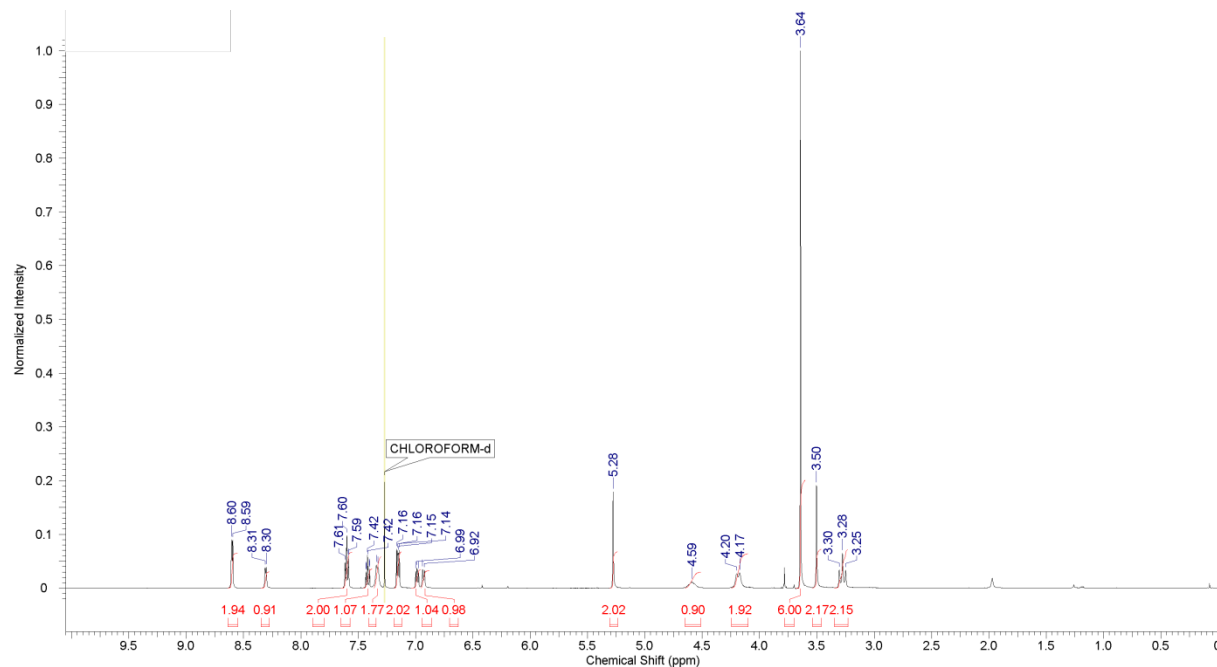


¹³C NMR of *trans* isomer: **2'** – DEPT : (S = solvent)

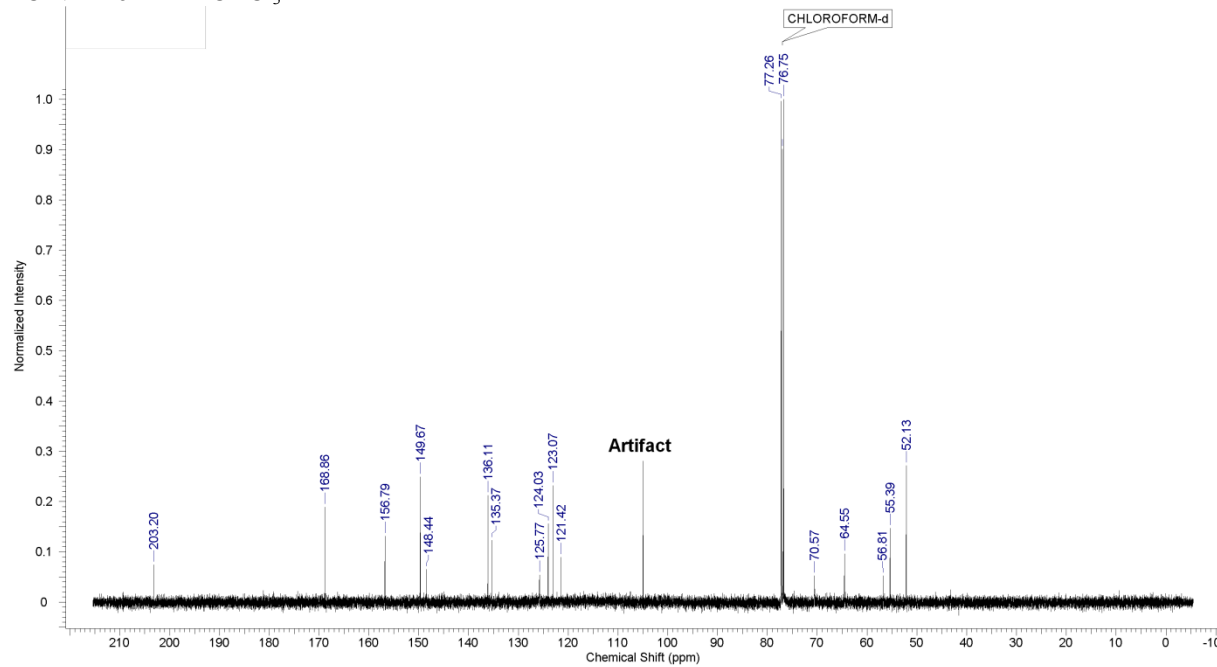


L4: (2R,4S)-dimethyl 9-oxo-2,4-di(pyridin-2-yl)-3-(pyridin-2-ylmethyl)-3,7-diazabicyclo[3.3.1]nonane-1,5-dicarboxylate.

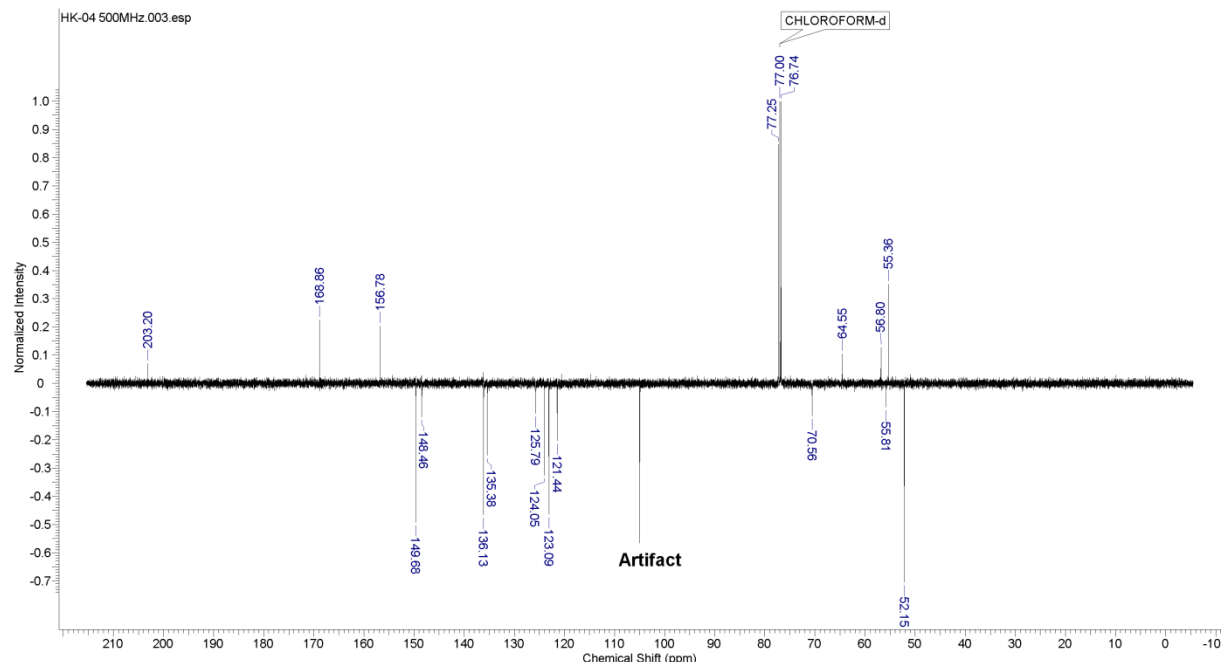
¹H NMR of L4 in CDCl₃:



¹³C NMR of L4 in CDCl₃



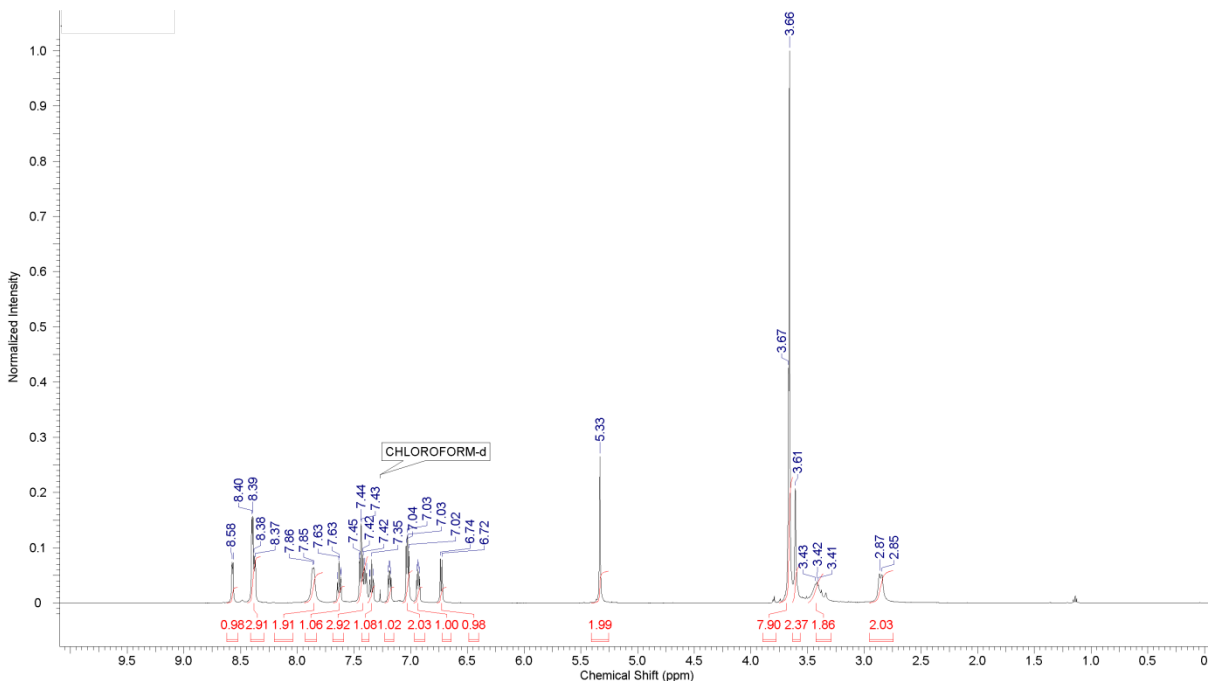
jmod ^{13}C NMR of **L4** in CDCl_3 :



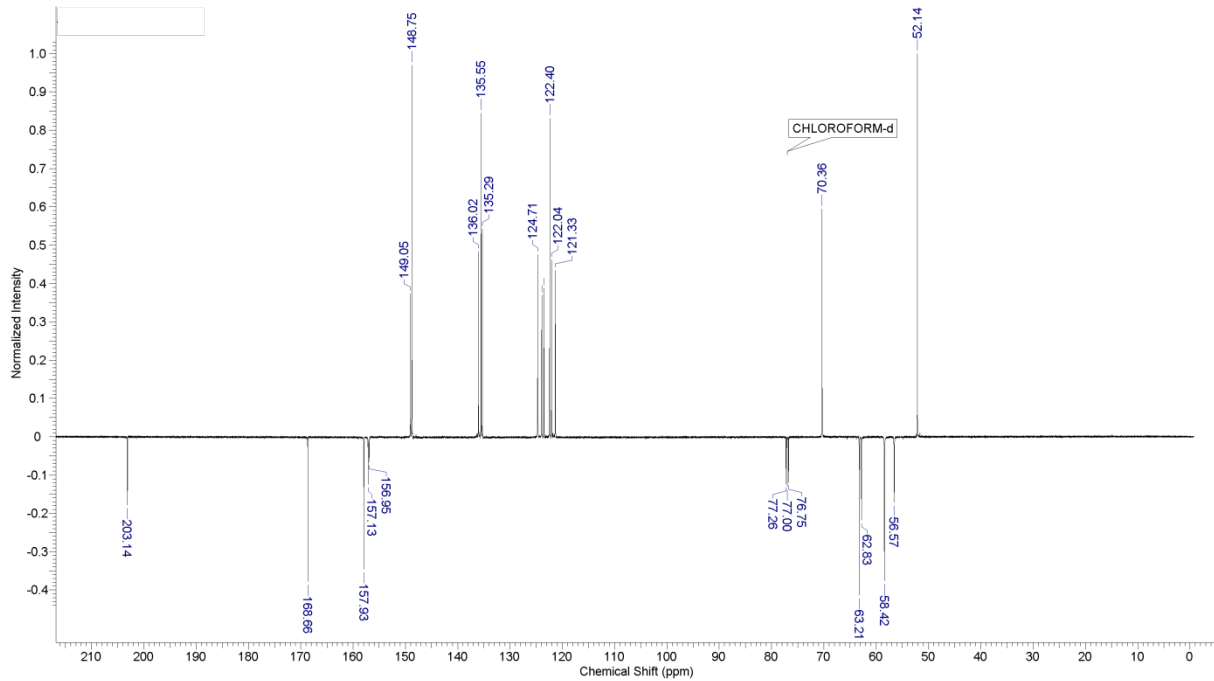
L1: (2R,4S)-dimethyl 9-oxo-2,4-di(pyridin-2-yl)-3,7-bis(pyridin-2-ylmethyl)-3,7-diazabicyclo[3.3.1]nonane-1,5-dicarboxylate

To a refluxed solution of (2S,6R)-dimethyl 4-oxo-2,6-di(pyridin-2-yl)-1-(pyridin-2-ylmethyl)piperidine-3,5-dicarboxylate (5.814 g; 12.6 mmol) in tetrahydrofuran formaldehyde (37% solution in H₂O) (2.451 g; 30.2 mmol; 2.4 eq) and 2-(aminomethyl)pyridine amine (1.633 g; 15.1 mmol; 1.2 eq) were added. Then the reaction was stopped after 1h and all volatiles were evaporated under reduced pressure. The residue was dissolved in *iso*-propanol and after the addition of diethyl ether the solution was left overnight in room temperature. The resulting white, crystalline solid was filtered off and washed with diethyl ether yielding 0.556 g of a pure *cis*-isomer. The subsequent workup of the remaining filtrate yielded 3.565 g of a pure trans isomer which was refluxed in 95% ethanol (50 ml) for 4h. Then, the volatiles were removed under reduced pressure and the pure *cis* isomer was crystallised from *iso*-propanol / diethyl ether solution and combined with a first crop yielding together 1.196 g (16 %) of the desired product. ¹H NMR (500 MHz, CDCl₃): δ=2.86 (2H, t, *J*=9.78, *H*-6/8 eq.), 3.42 (2H, m, *H*-6/8 ax.), 3.61 (2H, s, N7-CH₂py), 3.66 (6H, s, -CO₂CH₃), 3.67 (2H, s, N3-CH₂py), 5.33 (2H, s, *H*-2/4), 6.73 (1H, d, *J*=6.85, N3-CH₂py-6), 6.94 (1H, dd, *J*=6.85, 4.89, N3-CH₂py-4), 7.03 (2H, dd, *J*=6.85, 4.89, CH₂py-4), 7.19 (1H, dd, *J*=6.85, 4.89, N7-CH₂py-4), 7.35 (1H, tm, *J*=7.83, N3-CH₂py-5), 7.40 (1H, d, *J*=7.82, N7-CH₂py-6), 7.44 (2H, td, *J*=7.82, 1.96, CH₂py-5), 7.63 (1H, tm, *J*=7.83, N7-CH₂py-5), 7.85 (2H, d, *J*=4.89, CH₂py-6), 8.38 (1H, d, *J*=4.89, N3-CH₂py-3), 8.40 (2H, d, *J*=3.91, CH₂py-3), 8.55 (1H, d, *J*=4.89, N7-CH₂py-3). ¹³C NMR (126MHz, CDCl₃): δ=52.1 (-CO₂CH₃), 56.6 (N3-CH₂py), 58.4 (C-6/8), 62.83 (C-1/5), 63.2 (N7-CH₂py), 70.4 (C-2/4), 121.3 (N3-CH₂py-4), 122.0 (N7-CH₂py-4), 122.4 (CH₂py-4), 123.5 (N3-CH₂py-6), 123.9 (N7-CH₂py-6), 124.7 (CH₂py-6), 135.3 (N3-CH₂py-5) 135.6 (CH₂py-5), 136.0 (N7-CH₂py-5), 148.8 (N3-CH₂py-3, CH₂py-3), 149.1 (N7-CH₂py-3), 157.0 (N3-CH₂py-1) 157.1 (N7-CH₂py-1), 157.9 (CH₂py-1), 168.7 (-CO₂CH₃), 203.1(C-9). HRMS (ESI): m/z calcd for C₃₃H₃₃N₆O₅: 593.2507 [M+H⁺]; found: 593.2492; elemental analysis calcd (%) for C₃₃H₃₂N₆O₅: C 66.88, H 5.44, N 14.18; found: C 66.02, H 5.48, N 14.14.

¹H NMR of **L1** in CDCl₃:



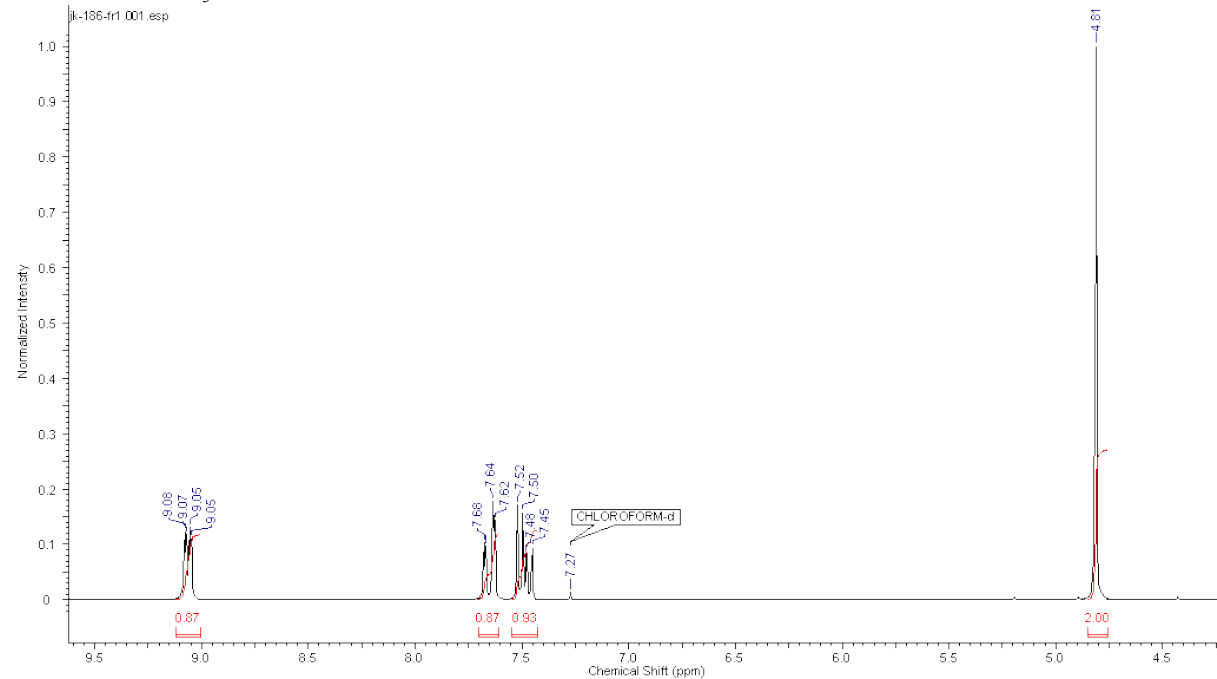
^{13}C NMR of **L1** (jmod) in CDCl_3 :



3-Chloromethylpyridazine:^[2]

To a refluxed solution of 3-methylpyridazine (1.000 g; 10.6 mmol) in chloroform (25 ml) trichloroisocyanuric acid (0.986 g; 4.2 mmol) was added in portions over 40 min. Then reaction was refluxed for 3 h, cooled down and reaction mixture filtered through a celite pad. The filtrate has been diluted with dichloromethane, washed with 1M NaOH (1 x 40 ml) and brine (1 x 40 ml), dried over Na₂SO₄ and solvent evaporated. The crude product was purified on Silica column (cyclohexane/ethyl acetate 2:1 and then 3:2) yielding pure 3-chloromethylpyridazine (158 mg; 12 %). The product was unstable on storage so it was used directly in the alkylation process (see below). ¹H NMR (200MHz, CDCl₃) δ_H 4.81 (2H, s, -CH₂Cl), 7.45 – 7.52 (1H, m, pdzH-6), 7.62 – 7.68 (1H, m, pdzH-5), 9.05 – 9.08 (1H, m, pdzH-4).

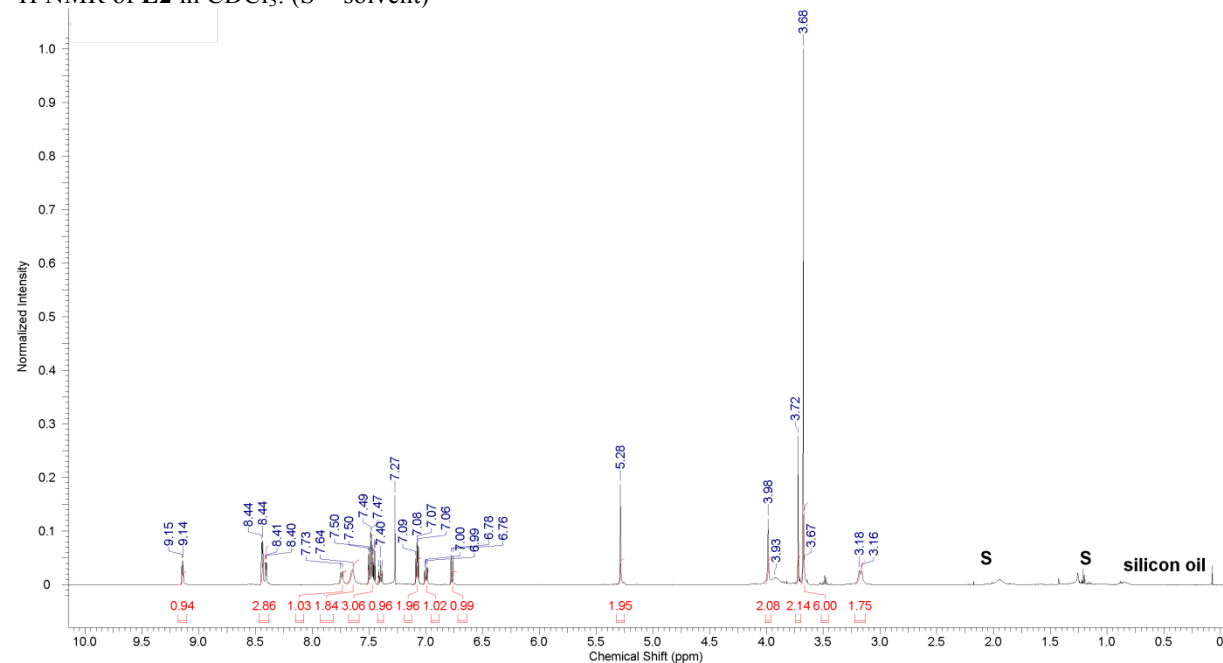
¹H NMR in CDCl₃



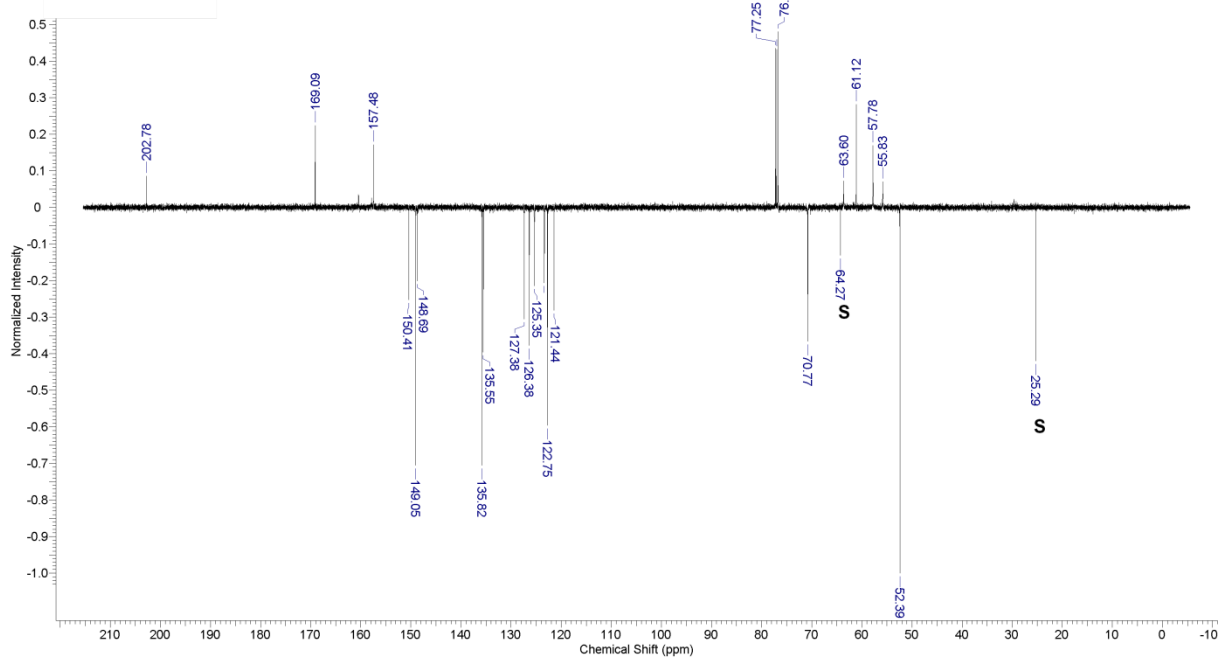
L2: (2R,4S)-dimethyl 9-oxo-7-(pyridazin-3-ylmethyl)-2,4-di(pyridin-2-yl)-3-(pyridin-2-ylmethyl)-3,7-diazabicyclo[3.3.1]nonane-1,5-dicarboxylate

To a solution of 3-(chloromethyl)pyridazine (129 mg; 1.00 mmol; 1.2 eq) in acetonitrile (15 ml) bispidinone **L4** (418 mg; 0.83 mmol; 1 eq) was added followed by the dropwise addition of N,N-diisopropylethylamine (190 mg; 1.47 mmol; 1.8 eq). Reaction was continued at room temperature for 72 h until a complete conversion of the main substrate. The solids were filtered and volatiles evaporated under reduced pressure. The residue was dissolved in chloroform and washed with brine and a saturated solution of NaHCO₃. The organic fraction was dried over anhydrous Na₂SO₄ and solvent evaporated. Obtained residue was purified by silica gel flash column chromatography (dichloromethane/*iso*-propanol 10:1) yielding 260 mg (53%) of a pure product as a white solid. ¹H NMR (500 MHz, CDCl₃): δ=3.17 (2 H, d, *J*=10.76, *H*-6/8 eq.) 3.68 (6 H, s, -CO₂CH₃) 3.72 (2 H, s, N3-CH₂pyridine(py)) 3.91 (2 H, br. s., *H*-6/8 ax.) 3.98 (2 H, s, N7-CH₂pyridazine(pdz)) 5.28 (2 H, s, *H*-2/4) 6.77 (1 H, d, *J*=7.83, N3 N3-CH₂py-6) 7.00 (1 H, dd, *J*=6.85, 4.89, N3-CH₂py-4) 7.08 (2 H, dd, *J*=7.82, 4.89, CH₂py-4) 7.36 – 7.41 (1 H, m, N3-CH₂py-5) 7.44 – 7.52 (3 H, m, N7-CH₂pdz-5, CH₂py-5) 7.64 (2 H, br. s., CH₂py-6) 7.74 (1 H, d, *J*=7.83, N7-CH₂pdz-6) 8.41 (1 H, d, *J*=3.91, N3-CH₂py-3) 8.44 (2 H, d, *J*=2.93, CH₂py-3) 9.14 (1 H, d, *J*=3.91, N7-CH₂pdz-4). ¹³C NMR (126MHz, CDCl₃): δ=52.4 (-CO₂CH₃), 55.83 (N3-CH₂pyridine), 57.78 (*C*-6/8), 61.12 (N7-CH₂pyridazine) 63.6 (*C*-1/5), 70.8 (*C*-2/4), 121.4 (N3-pi *C*-4), 122.8 (CH₂py-4), 123.4 (N3-CH₂py-6), 125.4 (CH₂py-6), 126.4 (N7-CH₂pdz-5) 127.4 (N7-CH₂pdz-6), 135.6 (N3-CH₂py-5) 135.8 (CH₂py-5), 148.7 (N3-CH₂py-3), 149.1 (CH₂py-3), 150.4 (N7-CH₂pdz-4), 157.5 (CH₂py-1) 157.9 (N3-CH₂py-1) 160.5 (N7-CH₂pdz-1), 169.1 (-CO₂CH₃), 202.8(*C*-9). HRMS (ESI) m/z calcd for C₃₂H₃₂N₇O₅: 594.2459 [M+H⁺]; found 594.2440.

¹H NMR of **L2** in CDCl₃: (S = solvent)



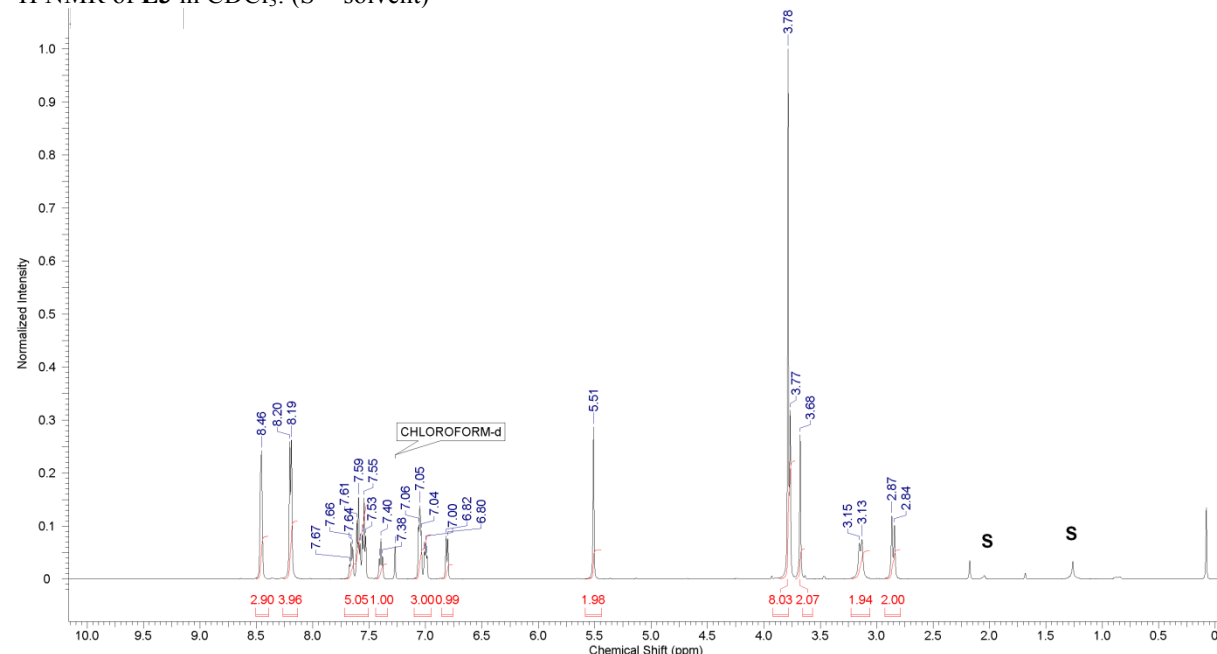
¹³C NMR of L2 (jmod) in CDCl₃: (S = solvent)



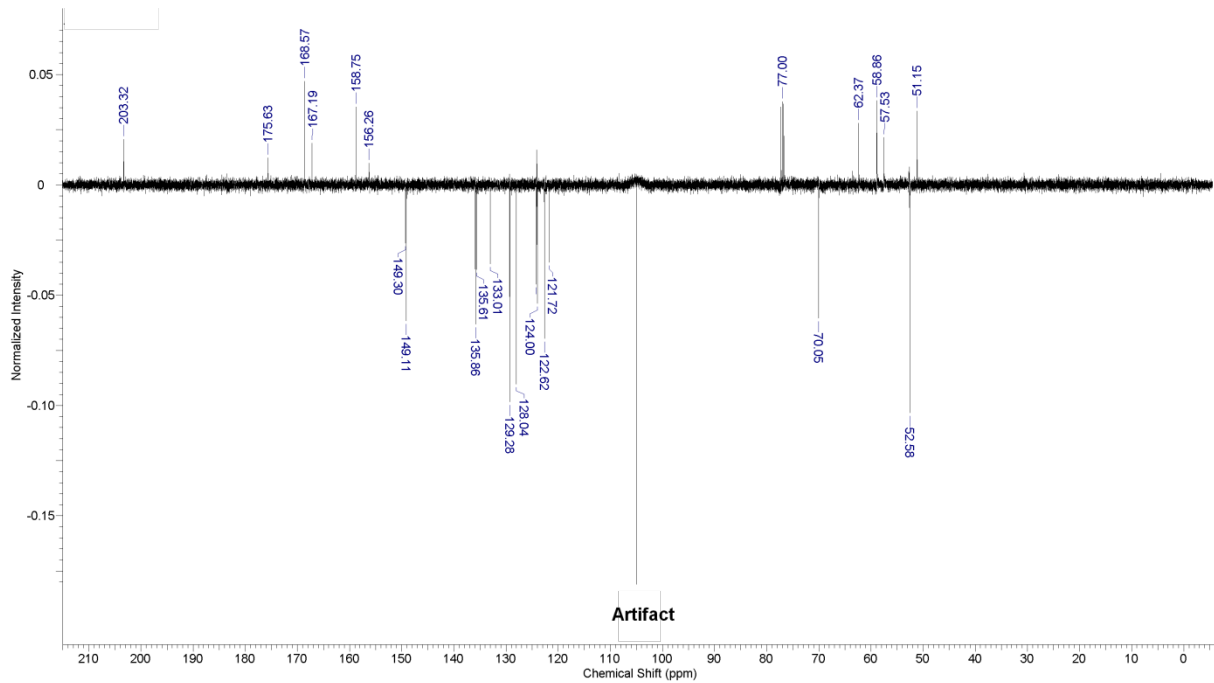
L3: (2R,4S)-dimethyl 9-oxo-7-((5-phenyl-1,2,4-oxadiazol-3-yl)methyl)-2,4-di(pyridin-2-yl)-3-(pyridin-2-ylmethyl)-3,7-diazabicyclo[3.3.1]nonane-1,5-dicarboxylate

To a solution of bispidinone **L4** (300 mg; 0.60 mmol) and 3-(chloromethyl)-5-phenyl-1,2,4-oxadiazole (131 mg; 0.67 mmol; 1.1 eq) in acetonitrile (30 ml) N,N-diisopropylethylamine (107 mg; 0.83 mmol; 1.4 eq) was added and reaction was refluxed for 24h. All volatiles were evaporated and the residue was redissolved in DCM and washed with brine and saturated solution of NaHCO₃. Organic phase was dried over anhydrous Na₂SO₄ and solvent was evaporated. The white solid crystallized from hot methanol (or methanol / diethyl ether mixture or *iso*-propanol) and was washed with methanol and diethyl ether yielding 136 mg (46%) of a pure product. Workup of the filtrate (crystallization from *iso*-propanol or methanol/diethyl ether mixture) yielded the additional material. ¹H NMR (500 MHz, CDCl₃): δ=2.85 (2 H, d, *J*=11.97, *H*-6/8 eq) 3.14 (2 H, d, *J*=11.11 Hz, *H*-6/8 ax) 3.68 (2 H s, N7-CH₂oxadiazole(oxdz)) 3.77 (2 H, s, N3-CH₂pyridine(py)) 3.78 (6 H, s, -CO₂CH₃) 5.51 (2 H, s, H-2,4) 6.81 (1 H, d, *J*=7.69 Hz, N3-CH₂py-6) 7.00 (1 H, t, *J*=5.98 Hz, N3-pi *H*-4) 7.02 - 7.04 (2 H, m, CHpy-4) 7.39 (1 H, t, *J*=7.27 Hz, N3-CH₂py-5) 7.54 (2 H, t, *J*=7.27 Hz, CHpy-5) 7.57 - 7.60 (2 H, m, Ar-3) 7.63 - 7.66 (1 H, m, Ar-4) 8.19 (4 H, d, *J*=7.69 Hz, Ar-2, CHpy-6) 8.46 (3 H, br. s., CHpy-3, N3-pi *H*-3). ¹³C NMR (126MHz, CDCl₃): δ=51.2 (N7-CH₂oxadiazole(oxdz)), 52.6 (-CO₂CH₃), 57.5 (N3-CH₂pyridine(py)), 58.9 (*C*-6/8), 62.4 (*C*-1/5), 70.0 (*C*-2/4), 121.7 (N3-CH₂py-4), 122.6 (CHpy-4), 124.0 (N3-CH₂py-6), 124.1 (Ar-1), 124.2 (CHpy-6), 128.0 (Ar-2), 129.3 (Ar-3), 133.0 (Ar-4), 135.6 (N3-CH₂py-5) 135.9 (CHpy-5), 149.1 (CHpy-3), 149.3 (N3-CH₂py-3), 156.3 (N3-CH₂py-1), 158.8 (CHpy-1) 167.2 (N7-CH₂oxdz-5), 168.6 (-CO₂CH₃), 175.6 (N7-CH₂oxdz-3) 203.3 (*C*-9). HRMS (ESI): m/z calcd for C₃₆H₃₄N₇O₅: 660.2565 [M+H⁺]; found 660.2529.

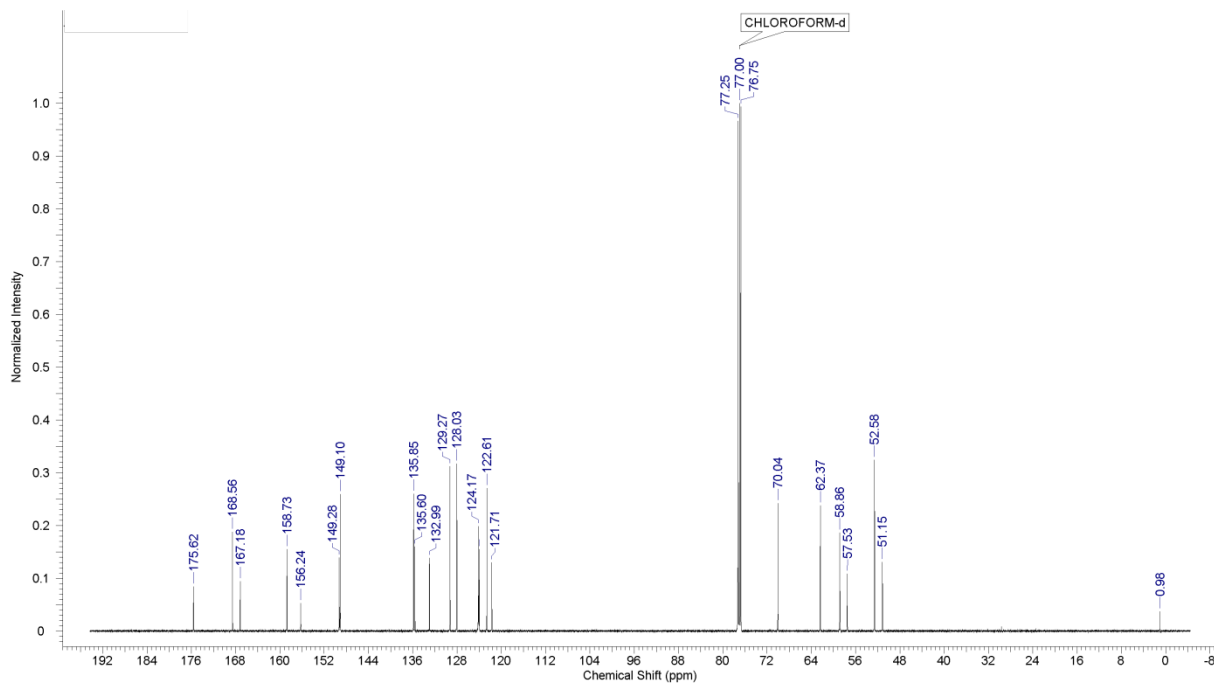
¹H NMR of **L3** in CDCl₃: (S = solvent)



^{13}C NMR of **L3** (jmod) in CDCl_3 :



^{13}C NMR of **L3** in CDCl_3 :



X-ray structural analyses of free ligands and ferrous complexes

Experimental

Suitable crystals were selected and mounted on a Gemini kappa-geometry diffractometer (Agilent Technologies UK Ltd) equipped with an Atlas CCD detector and using Mo ($\lambda = 0.7107 \text{ \AA}$) or Cu radiation ($\lambda = 1.5418 \text{ \AA}$).

Intensities were collected at low temperature by means of the CrysAlisPro software [1]. Reflection indexing, unit-cell parameters refinement, Lorentz-polarization correction, peak integration and background determination were carried out with the CrysAlisPro software [1]. An analytical absorption correction was applied using the modeled faces of the crystal. [2] The structures were solved by direct methods with SIR97 [3] and the least-square refinement on F^2 was achieved with the CRYSTALS software. [4]

All non-hydrogen atoms were refined anisotropically. The hydrogen atoms were all located in a difference map, but those attached to carbon atoms were repositioned geometrically. The H atoms were initially refined with soft restraints on the bond lengths and angles to regularize their geometry (C---H in the range 0.93--0.98 and N---H in the range 0.86--0.89 \AA) and $U_{\text{iso}}(\text{H})$ (in the range 1.2-1.5 times U_{eq} of the parent atom), after which the positions were refined with riding constraints.

For compound FeL3, the crystal structure displayed solvent accessible voids of 427 \AA^3 with delocalized electronic density. The contribution of this residual density was removed from the diffraction data with the SQUEEZE routine from the PLATON program [5] and led to an estimate of about 1.4 acetonitrile molecules per formula unit.

CCDC 827494 contains the supplementary crystallographic data for this paper. These data can be obtained free of charge from The Cambridge Crystallographic Data Centre via www.ccdc.cam.ac.uk/data_request/cif.

1 CrysAlisPro, Agilent Technologies, Version 1.171.34.49 (release 20-01-2011 CrysAlis171 .NET) (compiled Jan 20 2011, 15:58:25)

2 R.C. Clark, J.S. Reid *Acta Cryst.* **1995**, A51, 887-897.

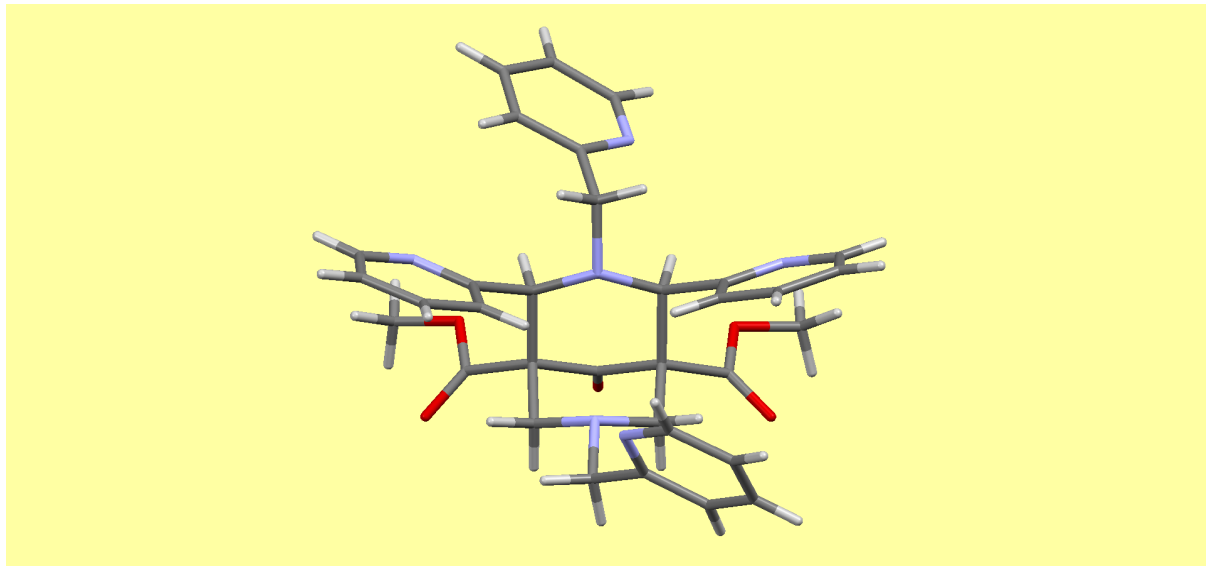
3 A. Altomare, M.C. Burla, M. Camalli, G.L. Cascarano, C. Giacovazzo, A. Guagliardi, A. Grazia, G. Moliterni, G. Polidori, R. Spagna *J. App. Cryst.* **1999**, 32, 115-119.

4 P.W. Betteridge, J.R. Carruthers, R.I. Cooper, K. Prout, D.J. Watkin *J. Appl. Cryst.* **2003**, 36, 1487.

5 A.L. Spek *Acta Cryst.* **2009**, D65, 148.

Figure S1 : L1 (CCDC 902550)

Crystals grown from iso-propanol / diethyl ether solvents' mixture.



Chemical formula : $C_{33}H_{32}N_6O_5$, $M_r = 592.65$ g.mol $^{-1}$, crystal dimensions : 0.46 x 0.59 x 0.71 mm, monoclinic system, space group $P2_1/c$, unit-cell dimensions : $a = 11.2852$ (9) Å, $b = 14.3962$ (9) Å, $c = 18.246$ (1) Å, $\alpha = 90^\circ$, $\beta = 104.565$ (8)° and $\gamma = 90^\circ$, $V = 2869.1$ (3) Å 3 , $Z = 4$, $\rho_{\text{calc}} = 1.372$ mg.m $^{-3}$, $\mu = 0.09$ mm $^{-1}$, Mo $K\alpha$ radiation, $\lambda = 0.7107$ Å, $T = 110$ K, $\theta_{\text{max}} = 29.5^\circ$, $\theta_{\text{min}} = 3.5^\circ$, no. of measured reflections : 21932, no. of independent reflections : 6995, $R_{\text{int}} = 0.038$, $R[F^2 > 2\sigma(F^2)] = 0.053$, $wR(F^2) = 0.125$, $\Delta\rho_{\text{max}} = 0.44$ e.Å $^{-3}$; $\Delta\rho_{\text{min}} = -0.38$ e.Å $^{-3}$

Figure S2 : FeL1 (CCDC 902554)

Crystals grown by diethyl ether diffusion into wet (5% v/v of H₂O) acetonitrile solution.

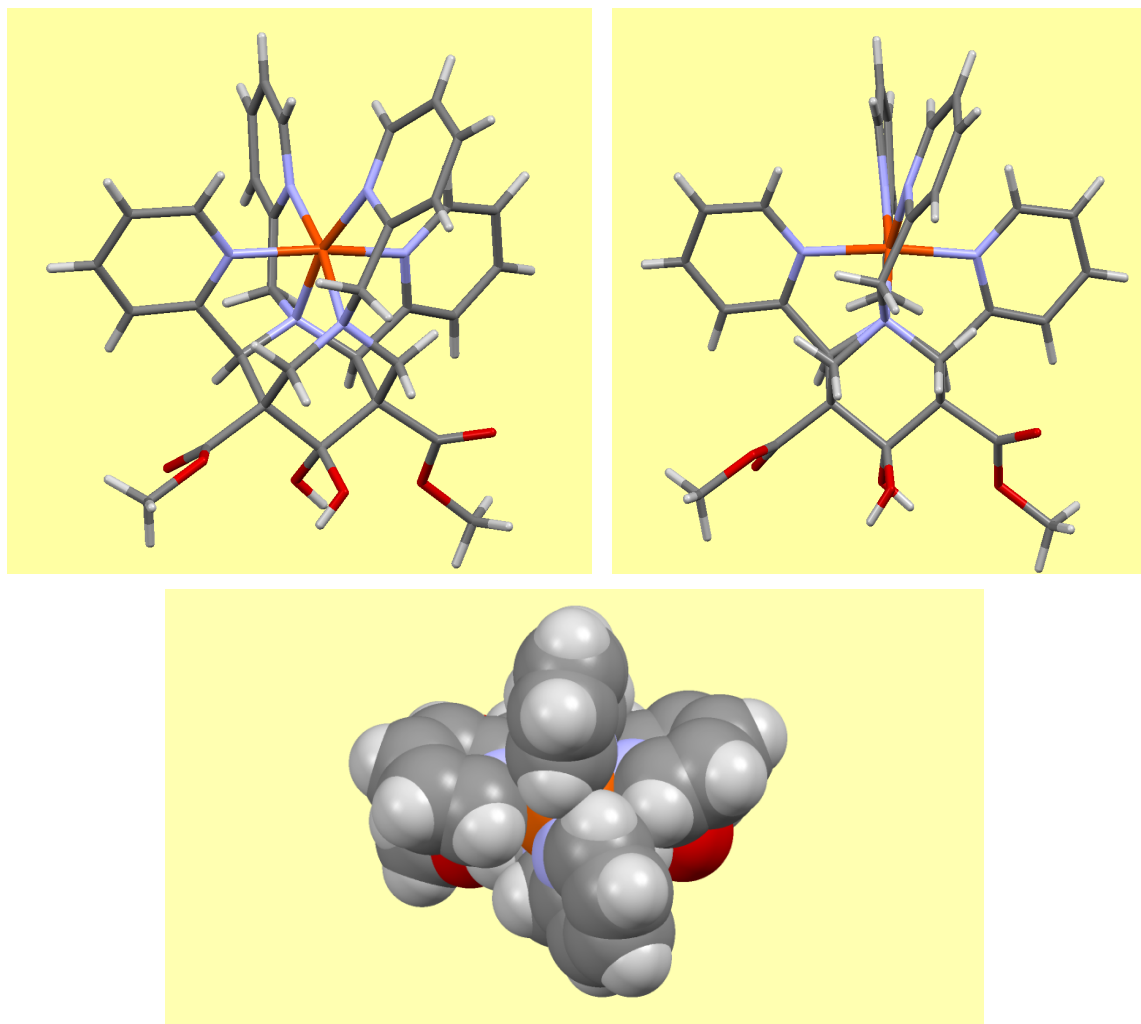


Figure S3 : FeL2 (CCDC 902552)

Crystals grown by diethyl ether diffusion into wet (5 % v/v of H₂O) acetonitrile solution.

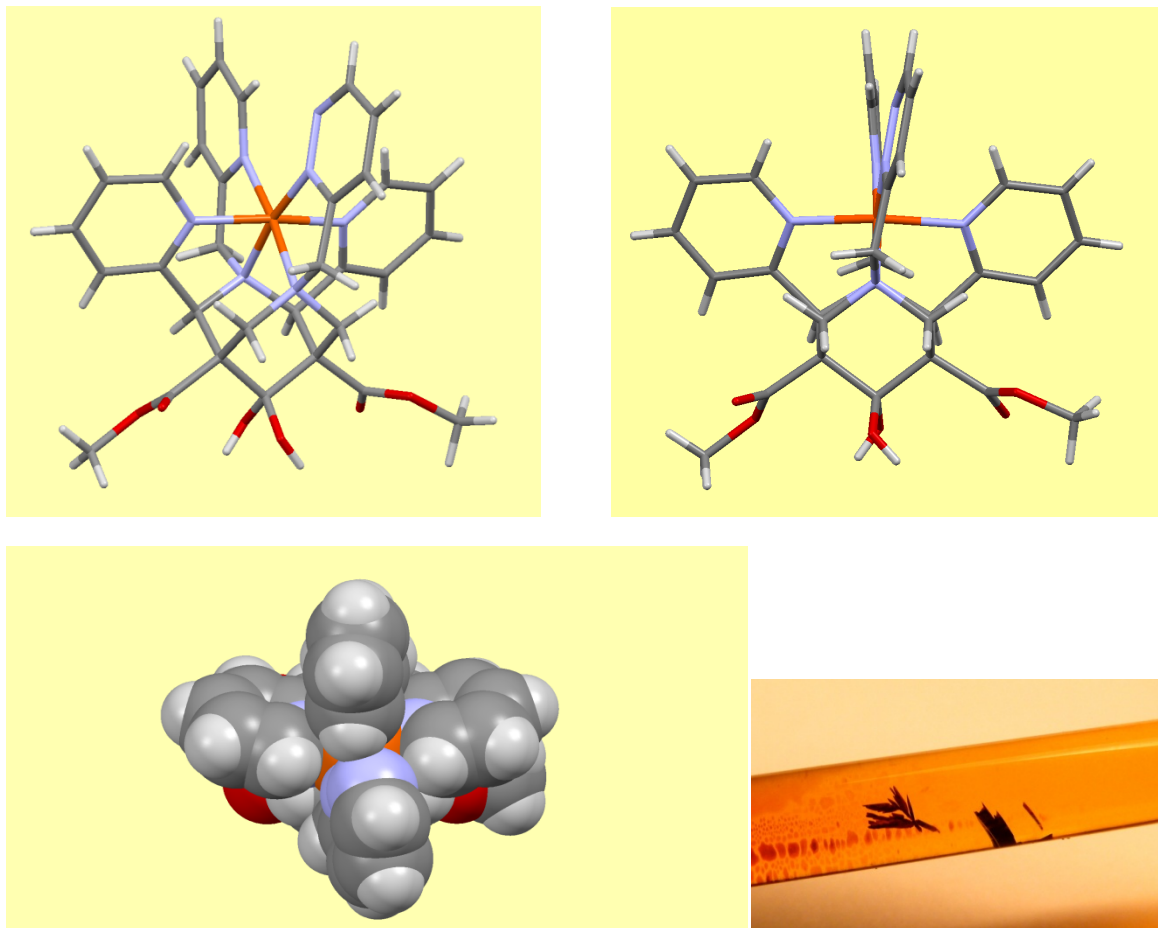


Figure S4 : FeL4(CH₃CN) (CCDC 902553)

Crystals grown by diethyl ether diffusion into acetonitrile solution.

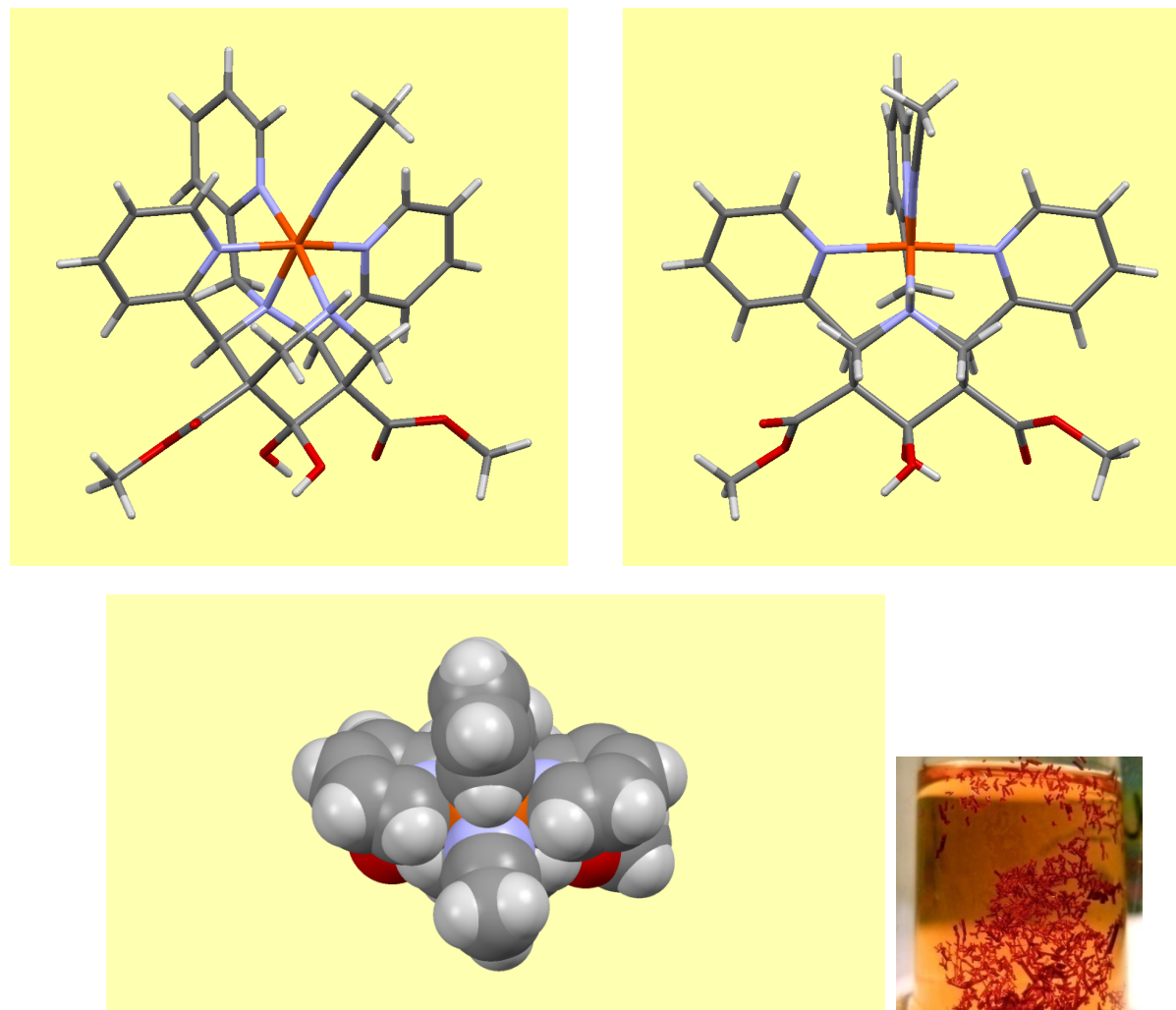


Figure S5 : FeL4(SO₄) (CCDC 902296)

Crystals grown by diethyl ether diffusion into methanol solution.

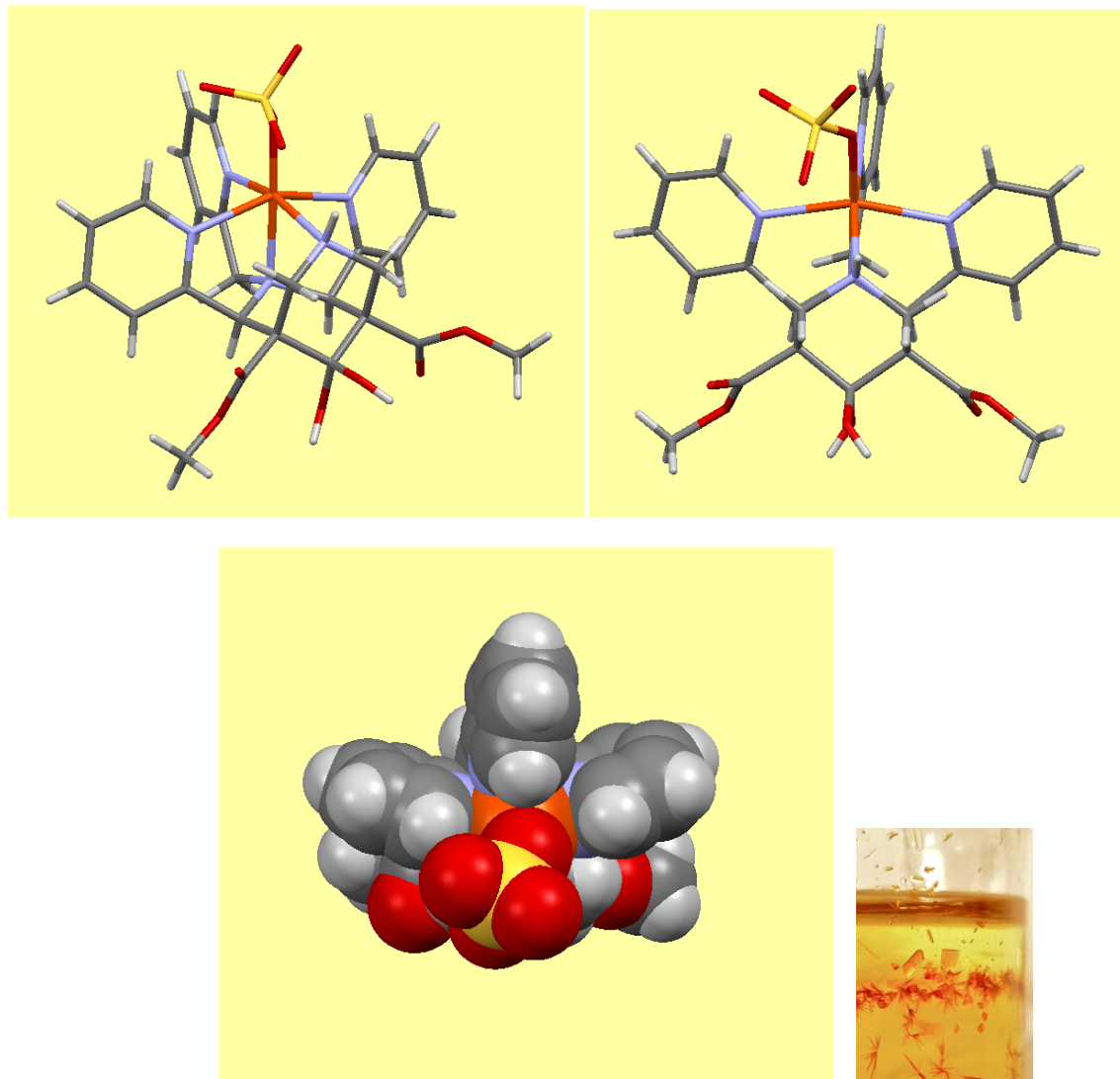
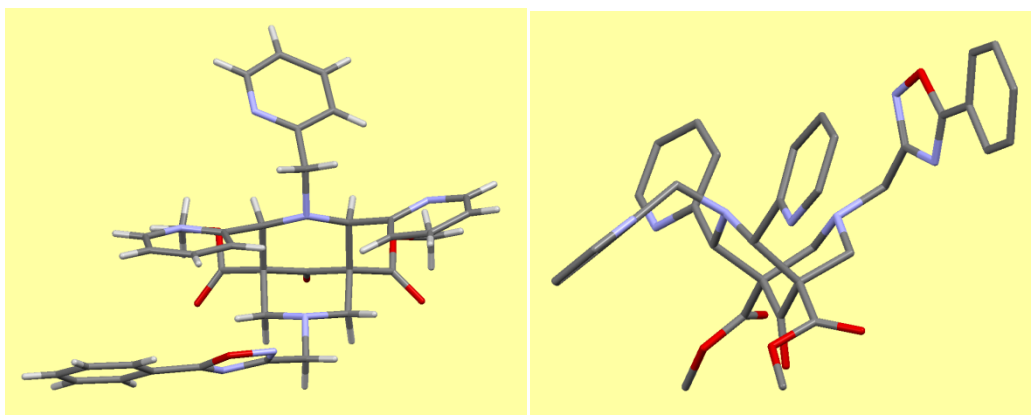


Figure S6 : L3 (CCDC 902551)

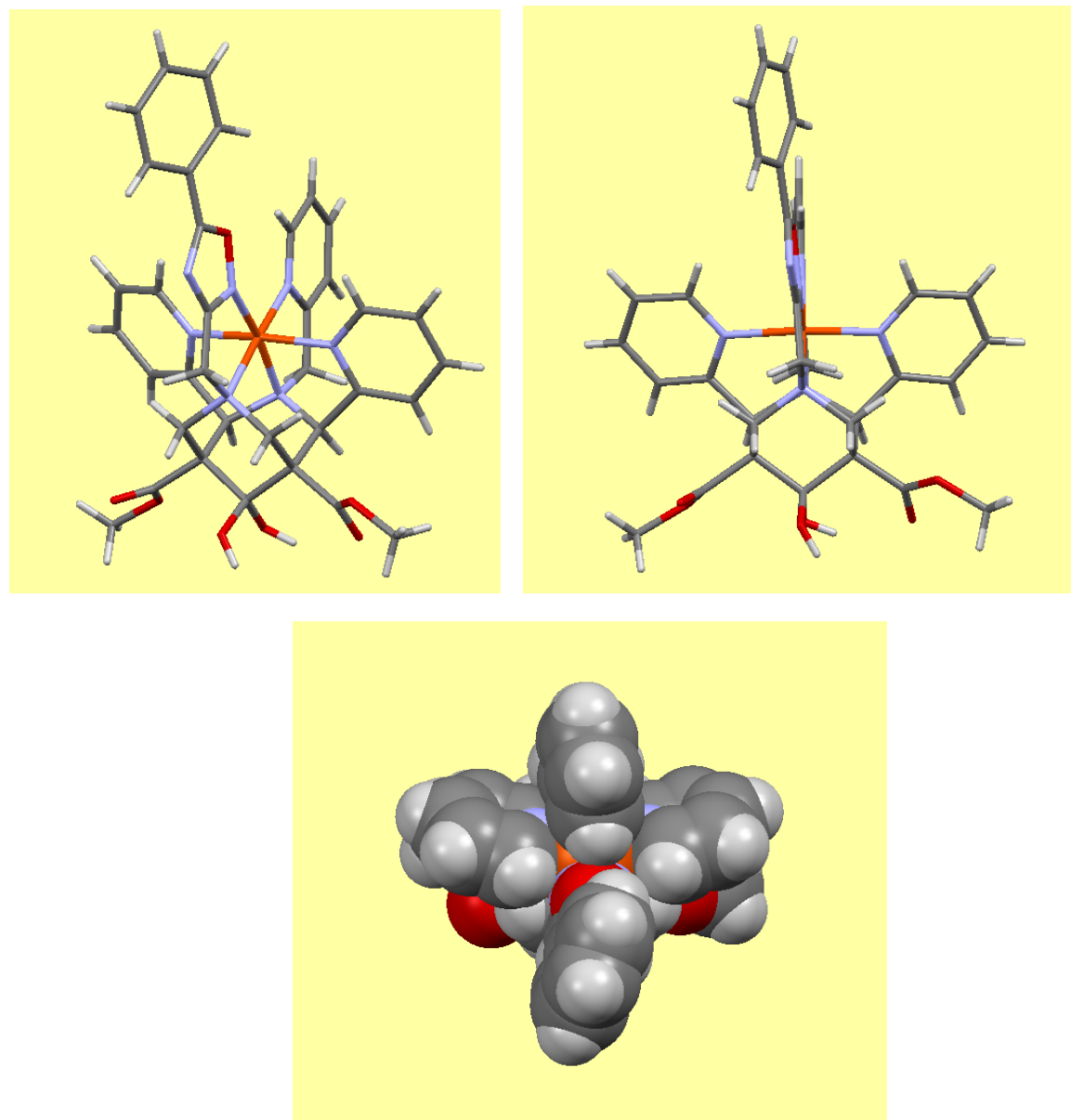
Crystals grown from iso-propanol.



Chemical formula : $C_{36}H_{33}N_7O_6$, $M_r = 659.70$ g.mol $^{-1}$, crystal dimensions : 0.182 x 0.222 x 0.533 mm, monoclinic system, space group $P2_1/c$, unit-cell dimensions : $a = 9.8633(8)$ Å, $b = 15.327(1)$ Å, $c = 21.604(2)$ Å, $\alpha = 90^\circ$, $\beta = 95.087(8)^\circ$ and $\gamma = 90^\circ$, $V = 3253.1(5)$ Å 3 , $Z = 4$, $\rho_{\text{calc}} = 1.347$ mg.m $^{-3}$, $\mu = 0.77$ mm $^{-1}$, Cu $K\alpha$ radiation, $\lambda = 1.5418$ Å, $T = 110$ K, $\theta_{\text{max}} = 66.8^\circ$, $\theta_{\text{min}} = 3.5^\circ$, no. of measured reflections : 22896, no. of independent reflections : 5743, $R_{\text{int}} = 0.044$, $R[F^2 > 2\sigma(F^2)] = 0.046$, $wR(F^2) = 0.129$, $\Delta\rho_{\text{max}} = 0.30$ e.Å $^{-3}$; $\Delta\rho_{\text{min}} = -0.28$ e.Å $^{-3}$

Figure S7 : FeL3 (CCDC 904020)

Crystals grown by diethyl ether diffusion into wet (5 % v/v of H₂O) acetonitrile solution.



NMR spectra and magnetic moments of complexes

Experimental

Magnetic susceptibilities in water ($\text{H}_2\text{O}/\text{D}_2\text{O}$ 85:15) or acetonitrile- d_3 at 298 K were determined by the Evans Method.^[3] Evans magnetic moment determinations were carried out analogously to previously described methods using Bruker 500 MHz and coaxial NMR tube.^[4, 5] 2% t-BuOH was used as reference in both cases and 5 mM solutions of complexes were used unless otherwise stated. Despite differences in magnetic susceptibilities of various solvents, for diluted solutions (equal or below 15 mM) this parameter can be neglected together with the term including the difference between density of pure solvent and solution.^[6, 7] Varied temperature magnetic susceptibilities were corrected in respect to the effect of solvent volume expansion/contraction upon heating/cooling (modified values of solvent densities at different temperatures were applied to calculate the real concentration of the analyte at different conditions).^[8] For deuterated solvents, correction parameters were used, which were calculated by dividing the density of the deuterated solvent by density of non-deuterated analogue at the temperature of sample preparation (298 K).^[9] No diamagnetic corrections were used for paramagnetic compounds. However, they can be evaluated either 1.) by using this same procedure to also determine the diamagnetic contribution for the corresponding diamagnetic complex with a different metal donor 2.) by use of Pascal's constants.

Thermodynamic parameters' estimation -fitting of experimental magnetic moments at different temperatures

The extraction of thermodynamic parameters was performed according to previous reports in many variants.^[4, 7, 10, 11] Experimental magnetic moment values can be fit to the following equation with four parameters to be optimised (μ_{LS} , μ_{HS} , ΔH° , ΔS°):

$$\mu_{\text{eff}} = \{\mu_{\text{LS}}^2[\exp(-\Delta H^\circ/RT)\exp(\Delta S^\circ/R) + 1]^{-1} + \mu_{\text{HS}}^2[\exp(\Delta H^\circ/RT)\exp(-\Delta S^\circ/R) + 1]^{-1}\}^{1/2} \quad (1)$$

where T is the temperature of the solution, μ_{eff} is the overall magnetic moment of the solution, μ_{LS} and μ_{HS} are the magnetic moments of respectively pure low-spin and a pure high-spin form of the complex investigated, ΔH° and ΔS° are respectively standard enthalpy and entropy of the spin transition process and R is the gas constant.

In case when the values of μ_{LS} and μ_{HS} are known, the fitting procedure involves only two parameters and hence leads usually straightforward to the solution.^[12] When the magnetic moments of the pure low-spin and or pure high-spin forms were not yet reported and the temperature range available, determined by the solvent, does not allow for pushing the equilibrium to one of the limits (exclusively low-spin or high-spin form present), the four-parameter fit is required to estimate not only the enthalpy and entropy of the complex but also μ_{LS} and μ_{HS} . This fitting problem leads often to the high uncertainty^[4, 7] or even disables the reliable fit completely, especially when the amount of data is limited by the narrow range of available temperatures, being the case particularly for water solutions. Hence, the most obvious strategy is to make the assumptions concerning one of the parameters and fix it, leading to a much simpler and usually significantly less problematic three-parameter fit. One of the options would be to assume the magnetic moment of the low spin or a high spin form on the basis of the experimental data accessible for possibly most similar analogues. However, this requires a particular attention as the temperature-independent-paramagnetism, which is the most common reason for a deviation from the theoretical spin-only values of the magnetic susceptibility of complexes, can vary even among close analogues. Instead, the physically relevant assumptions on the extreme (minimum and maximum) values of μ_{HS} could be made as previously reported^[11] to rationalize the results: high spin magnetic moment was fixed to be either 4.9 (minimal value - spin-only value for iron with 4 unpaired electrons where $S = 2$: $\mu = [S(S+2)]^{1/2}$)^[13] or 5.4 (5.5 is a spin-only value of magnetic moment for species with 5 unpaired electrons and on the top of that great majority of the iron(II) high-spin complexes do not exceed this value).^[11]

For our purposes, two non-linear fit methods were used in order to find the optimal values of μ_{LS} , μ_{HS} , ΔH° and ΔS° describing the experimental data in the most reliable way, namely Levenberg-Marquardt algorithm and Generalized Reduced Gradient (GRG2) nonlinear optimisation code used by Microsoft Excel 2007 Solver add-in, according to the previously reported method (maximizing the R^2 of the fit and estimating the confidence intervals at 0.01 – Brown^[14] - as well as calculating the error according to the method proposed by Harris et al.^[15]

FeL1 => spin transition

Figure S8: ^1H NMR spectrum at in D_2O (298 K):

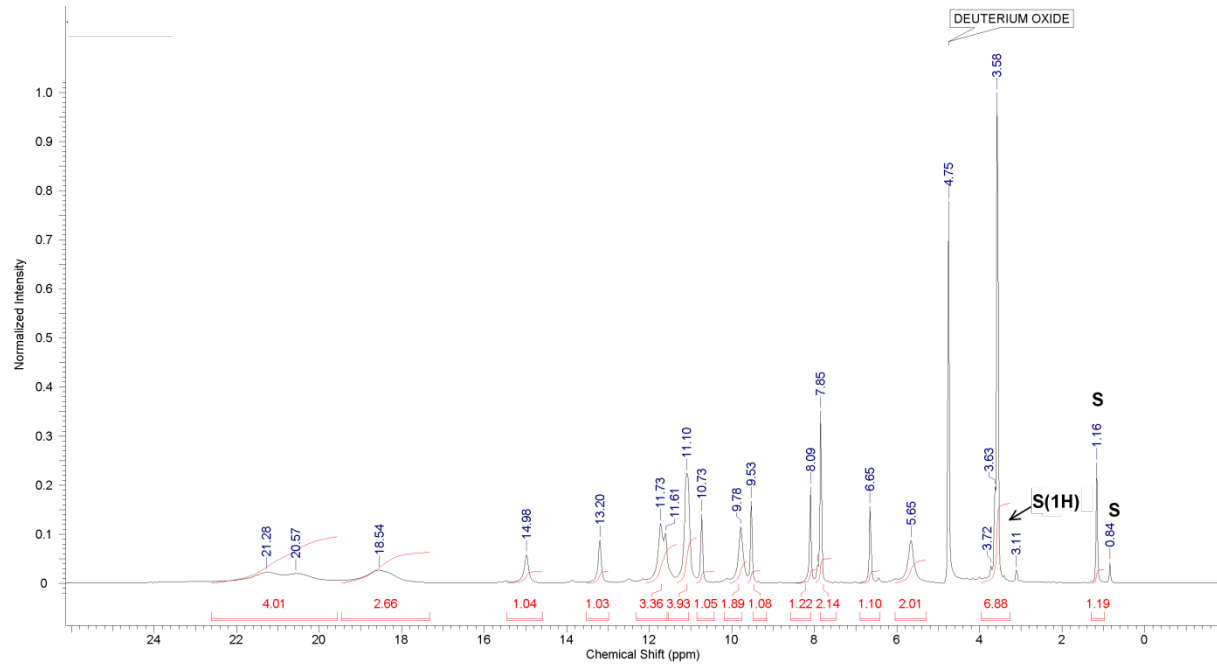


Figure S9: Comparison of FeL1 ^1H NMR spectra at RT (298 K) in different solvents:

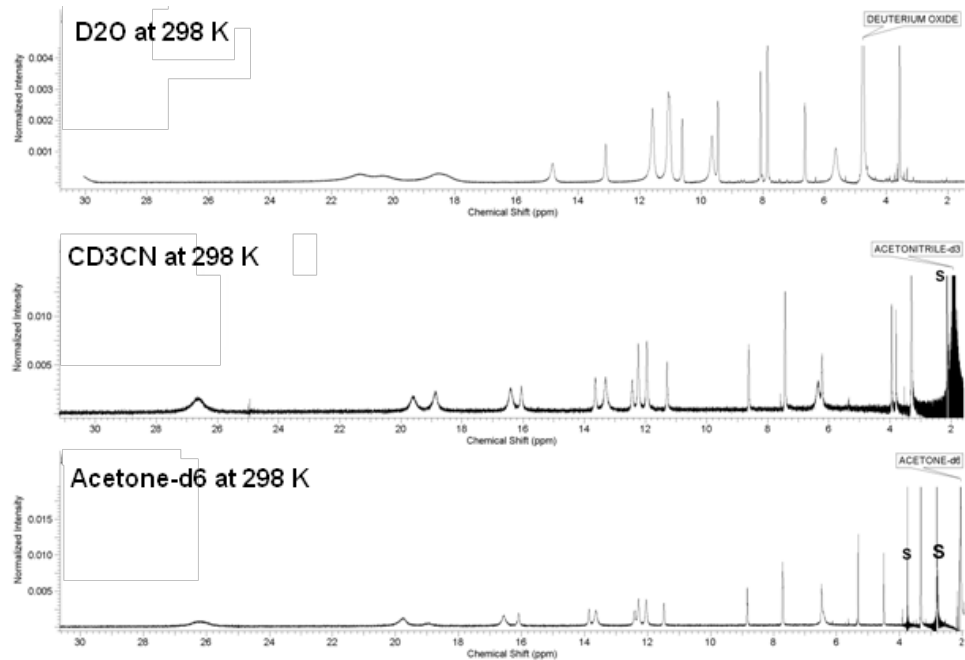


Figure S10: Variable temperature ^1H NMR spectra of FeL1 in D_2O (298 K – 353 K)

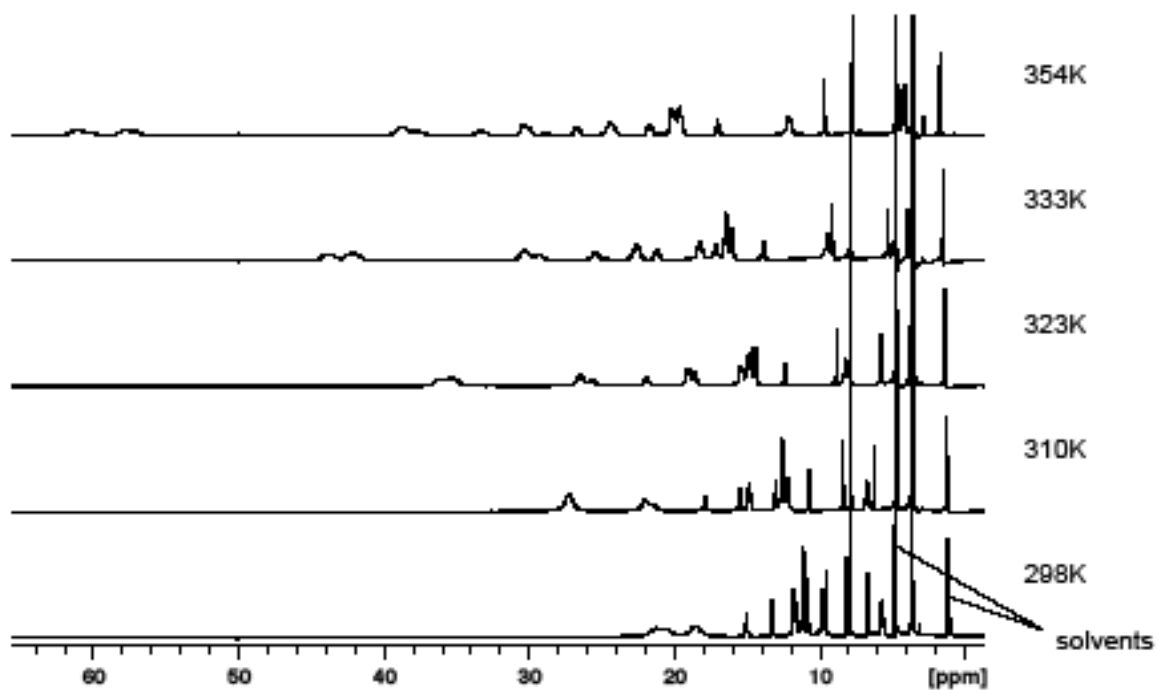
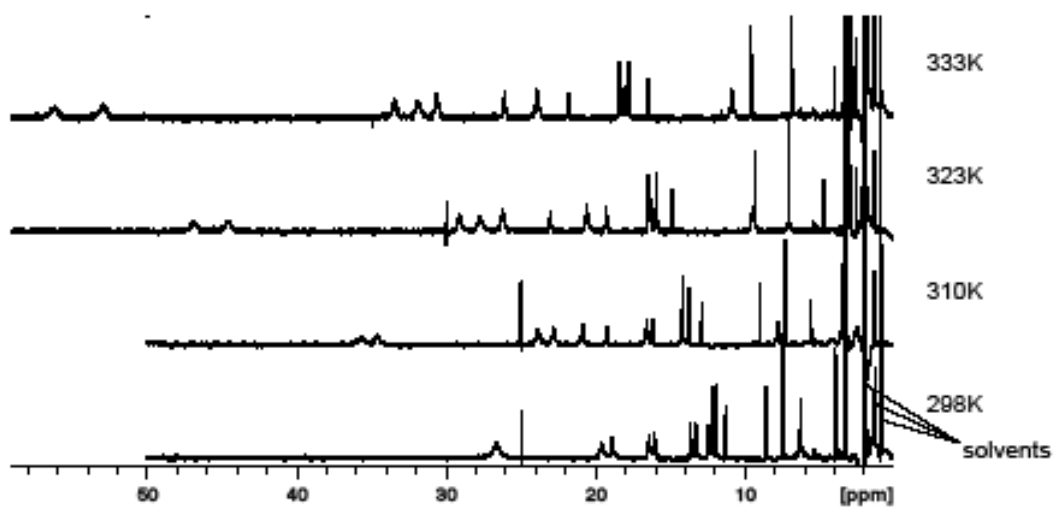


Figure S11 : Variable temperature ^1H NMR spectra of FeL1 in CD_3CN (233 K - 333 K)

a) 333 K – 298 K



b) 283 K – 233 K

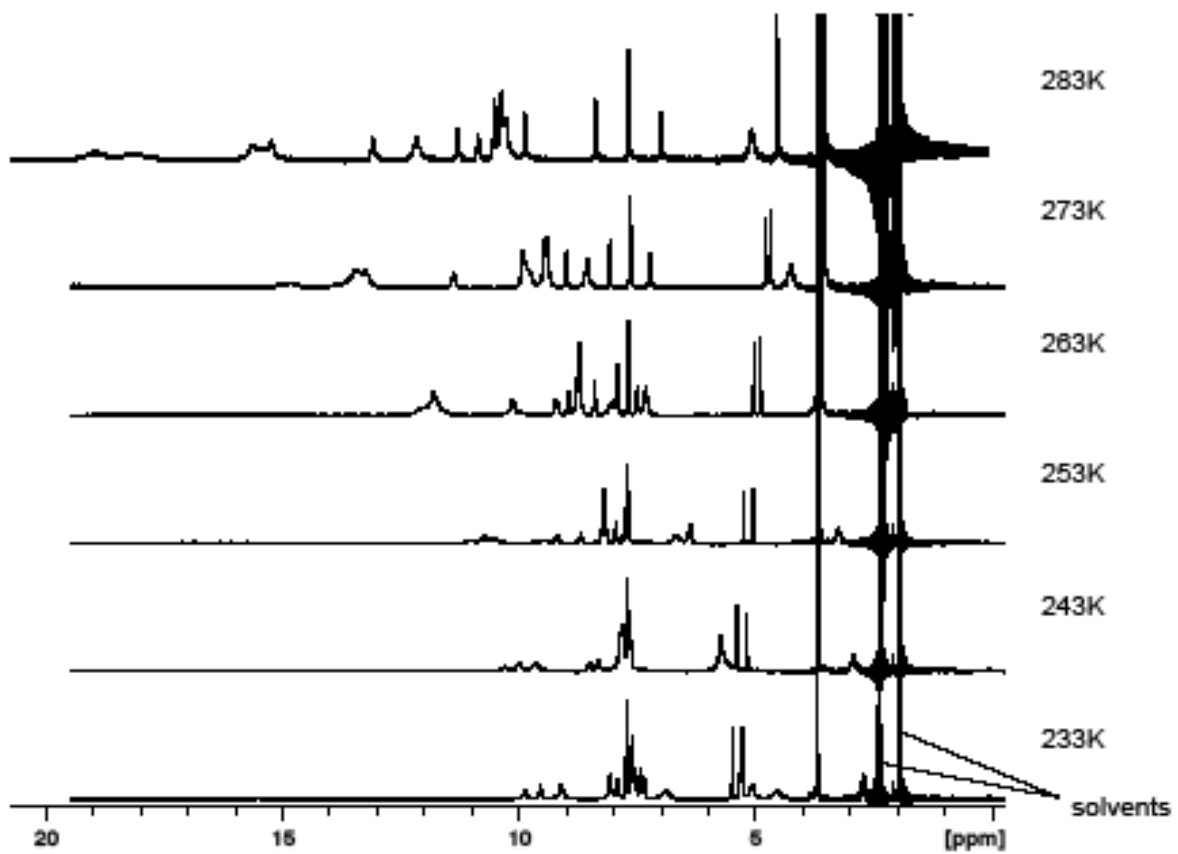


Figure S12 : Variable temperature ^1H NMR spectra in Acetone-*d*6 (213 - 323 K)

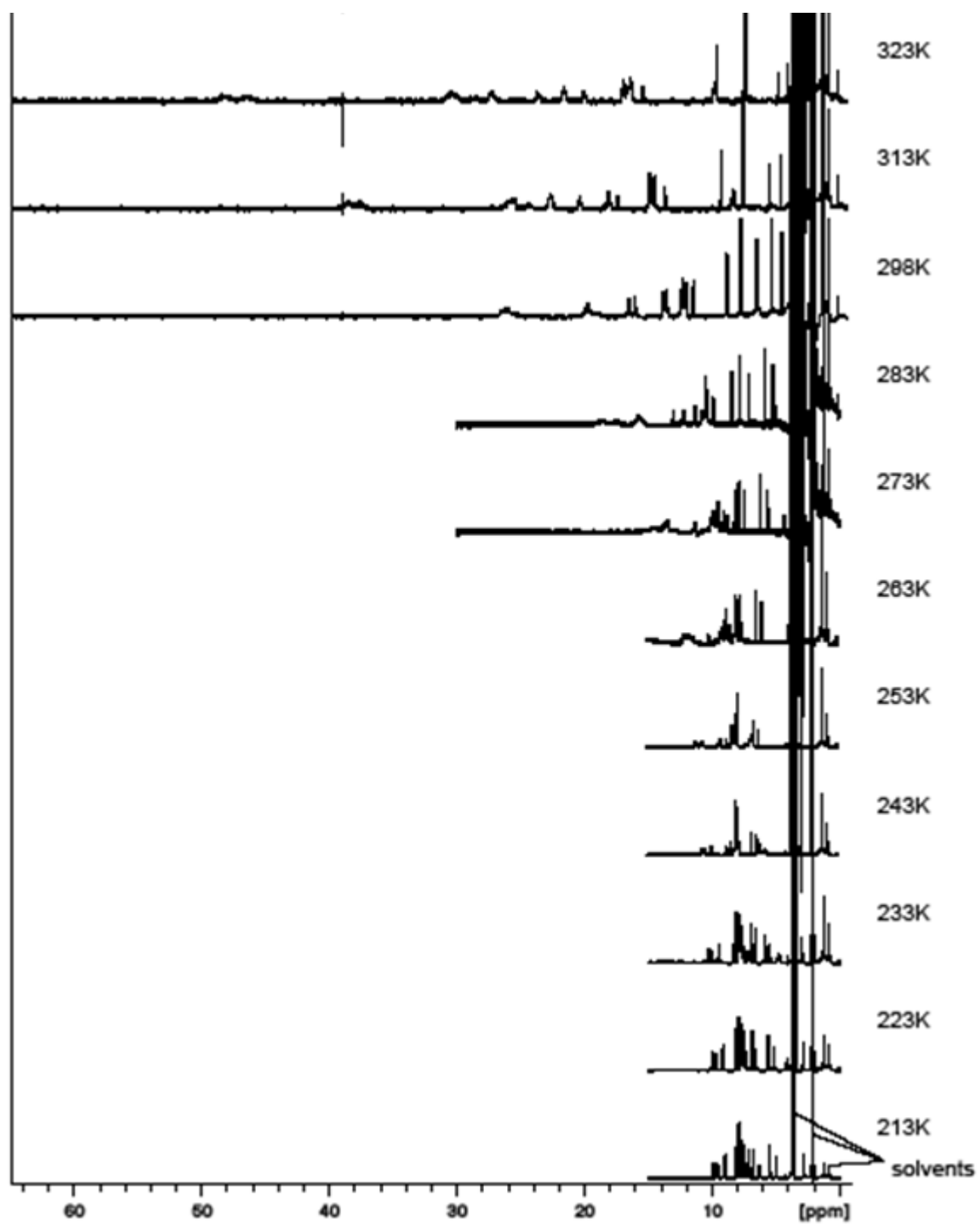
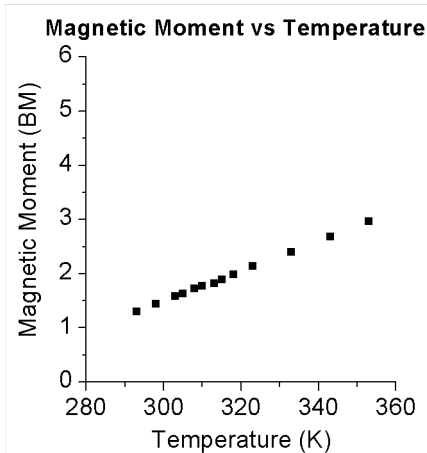


Figure S13. Magnetic moments of FeL1 (Evans' method) at different temp.

Temp. [K]	Magnetic Moment [BM]
293	1.31
298	1.44
303	1.59
305	1.64
308	1.73
310	1.78
313	1.82
315	1.90
318	1.98
323	2.14
333	2.40
343	2.68
353	2.96

FeL1 in aqueous solution



Temp. [K]	Magnetic Moment [BM]
253	0.80
258	0.87
263	0.98
268	1.10
273	1.22
278	1.29
283	1.38
288	1.51
293	1.64
298	1.77
303	1.93
308	2.11
313	2.25
318	2.37
323	2.56
328	2.65
333	2.82

FeL1 in acetonitrile-d3

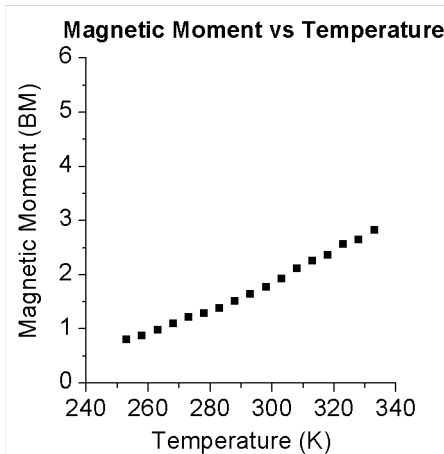


Figure S14. Nonlinear fitting curves of the spin transition of FeL1 in solution.

solvent	method	μ_{LS} [BM]	μ_{HS} [BM]	ΔH° [kJ/mol]	ΔS° [J/(mol*K)]	$T_{1/2}$ [K]
water	Solver (Newton's gradient)	0,00 ± 0,05	5,02 ± 0,51	28,11 ± 1,34	74,35 ± 6,28	378
	Levenberg-Marquardt	0,00 ± 36612*	4,88 ± 0,90	28,52 ± 6,17	76,24 ± 21,79	374
water	Solver (Newton's gradient)	0,06 ± 0,04	4,90**	28,47 ± 0,42	75,98 ± 1,28	375
	Levenberg-Marquardt	0,00 ± 37730*		28,34 ± 1,03	75,58 ± 2,86	375
water	Solver (Newton's gradient)	0,00 ± 0,05	5,40**	27,23 ± 0,22	70,13 ± 0,68	388
	Levenberg-Marquardt	0,00 ± 3488*		27,28 ± 1,03	70,29 ± 2,84	388
acetonitrile	Solver (Newton's gradient)	0,41 ± 0,13	5,40 ± 1,22	26,79 ± 2,93	72,15 ± 13,60	371
	Levenberg-Marquardt	0,40 ± 0,16	5,43 ± 1,21	26,72 ± 3,27	71,85 ± 14,54	372
acetonitrile	Solver (Newton's gradient)	0,46 ± 0,05	4,90**	28,18 ± 0,55	78,54 ± 1,66	359
	Levenberg-Marquardt	0,46 ± 0,06		28,16 ± 0,87	78,48 ± 2,66	359
acetonitrile	Solver (Newton's gradient)	0,41 ± 0,05	5,40**	26,80 ± 0,53	72,18 ± 1,59	371
	Levenberg-Marquardt	0,41 ± 0,08		26,79 ± 0,81	72,14 ± 2,47	371

* abnormally large uncertainty is a sign of overparametrisation (to small part of the curve is covered by the experimental data)

** fixed value of the magnetic moment of the high-spin form allows for a 3-parameter fit which leads to lower systematic uncertainties

In the case of acetonitrile solution of FeL1, data obtained from the measurements within the temperature range of 253 – 333 K were fit by the above-mentioned algorithms (Levenberg-Marquardt and Generalized Reduced Gradient nonlinear optimisation code used by Microsoft Office Excel's Solver add-in) leading to the comparable values of thermodynamic parameters. As a control, the same methods were applied to fit experimental data into the equation (1) but with μ_{HS} fixed at 4,9 and 5,4.^[11] In the case of aqueous solution of FeL1 the attempts to perform a non-linear fitting by the Levenberg-Marquardt method in all cases (including those with fixed μ_{HS}) always led to abnormally high errors of the μ_{LS} , suggesting an overparametrization (* in the table above). It can indicate that the data could suffer from the excessive number of parameters to be fit with covering only a small part of the curve, hence suggesting, that some assumptions considering at least one of the parameters should be made to decrease the number of flexible parameters. On the other hand, Solver supported optimisation, performed as described previously^[14] furnished reasonable values of the parameters. Three parameter-fits were also performed on experimental data from aqueous solution. All results are included in the table above.

FeL2 => low-spin

Figure S15: ^1H NMR spectrum of FeL2 in D_2O (298 K):

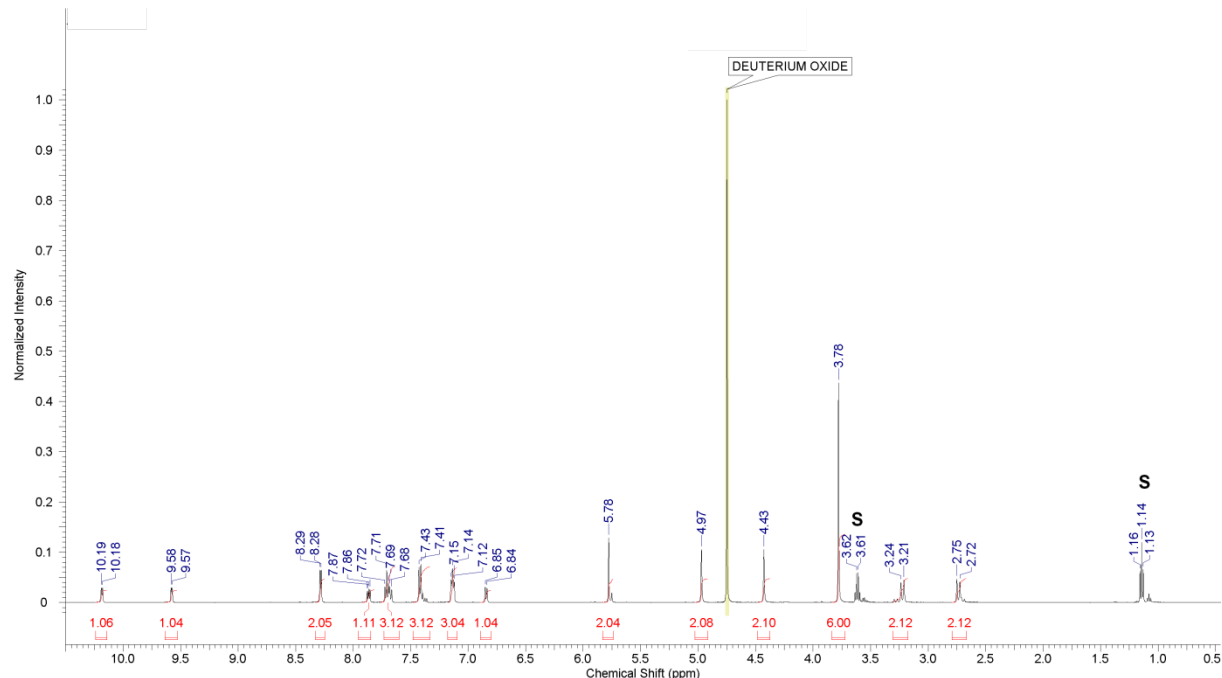


Figure S16: Comparison of ^1H NMR spectra of FeL2 at different temperatures (D_2O):

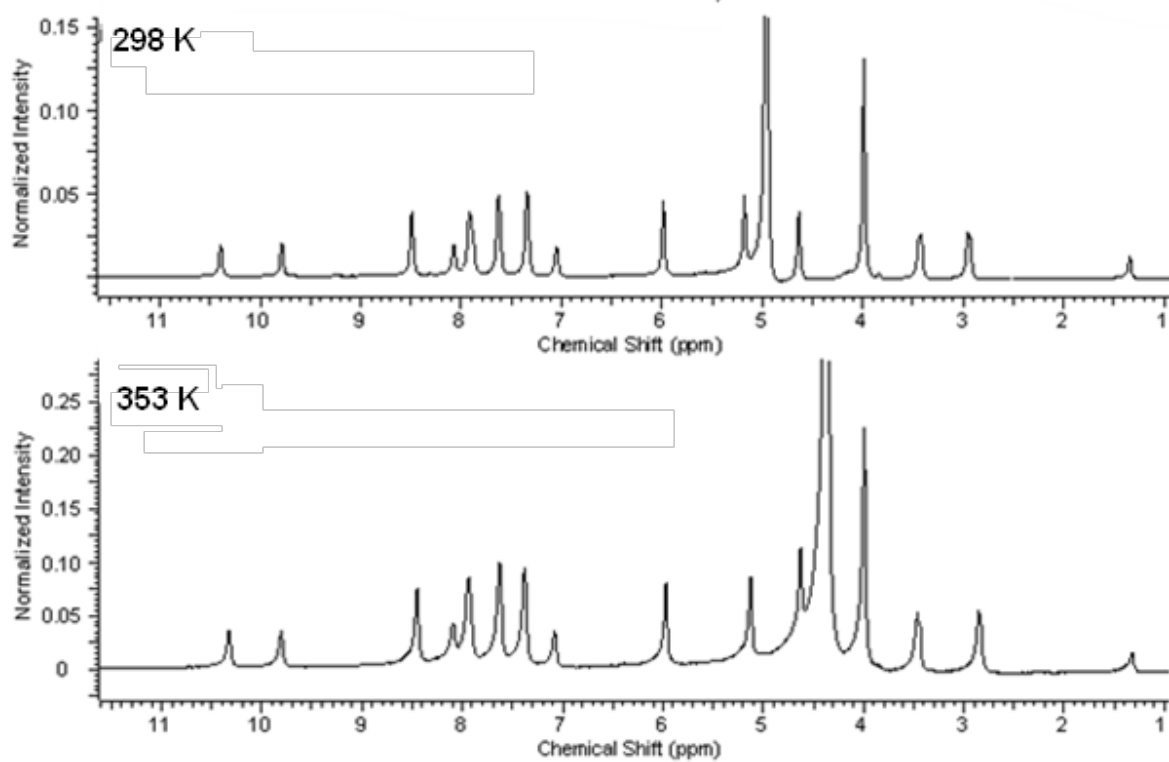
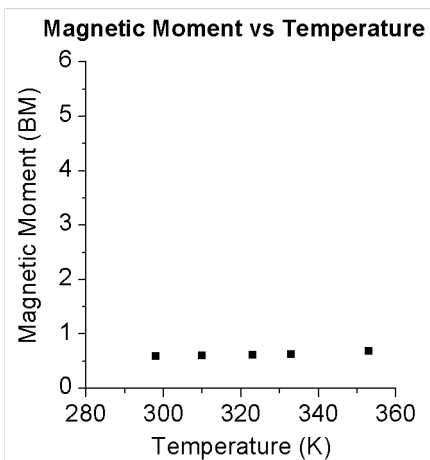


Figure S17: Magnetic moments of FeL2 (Evans' method) at different temperatures

FeL2 in aqueous solution

Temp. [K]	Magnetic Moment [BM]
298	0,59
310	0,60
323	0,62
333	0,62
353	0,69



FeL3 => low-spin

Figure S18: ^1H NMR spectrum in D_2O

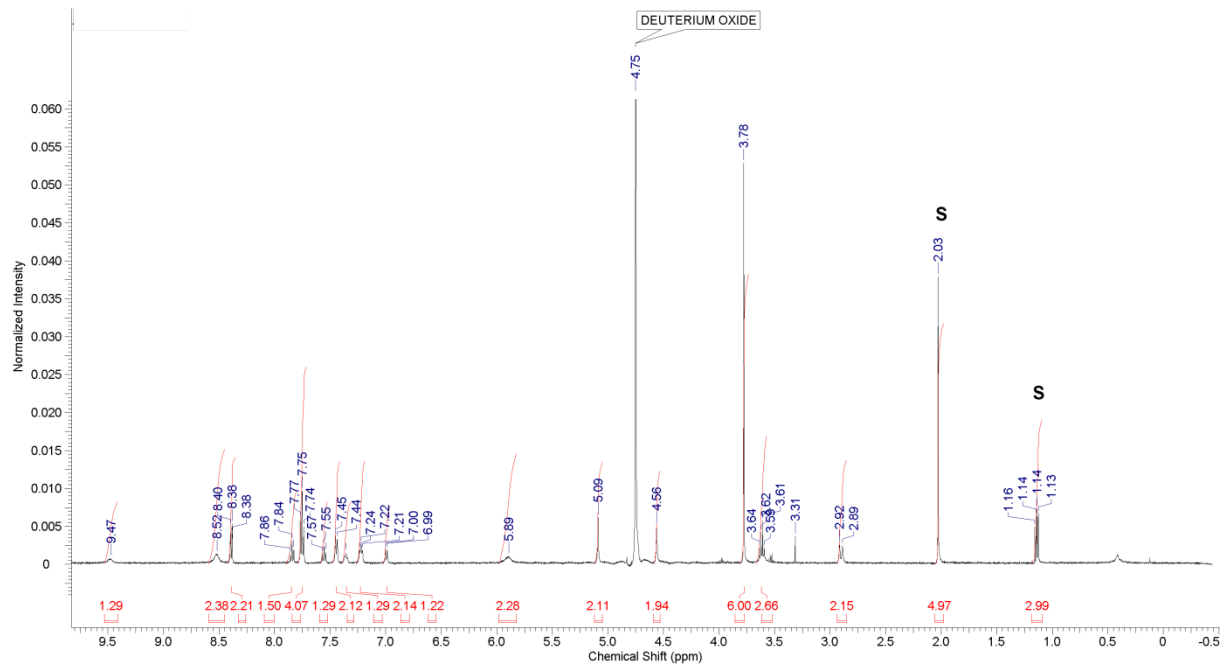


Figure S19: Temperature dependency (298 – 353 K) of ^1H NMR spectra in D_2O

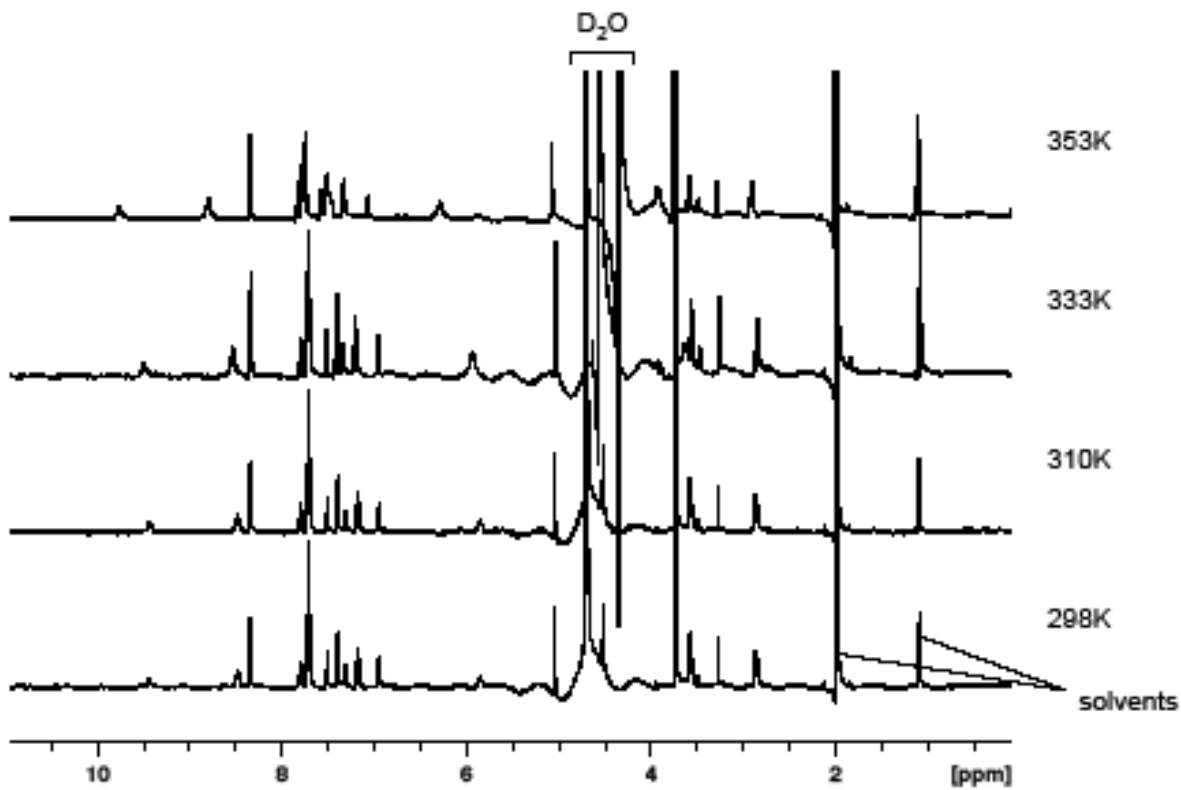
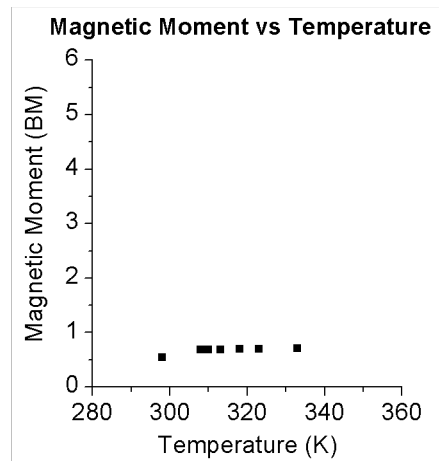


Figure S20: Magnetic moments of FeL3 (Evans' method) at different temperatures

Samples of 3,33 mM in H₂O/D₂O (85:15) : MeOD 2:1 were used due to solubility issues

FeL3 in aqueous solution

Temp. [K]	Magnetic Moment [BM]
298	0,54
308	0,68
310	0,69
313	0,68
318	0,70
323	0,70
333	0,71



FeL4(SO₄) => high spin

Figure S21 : ¹H NMR spectrum of Fe4(SO₄) in D₂O at 298 K (and zoom)

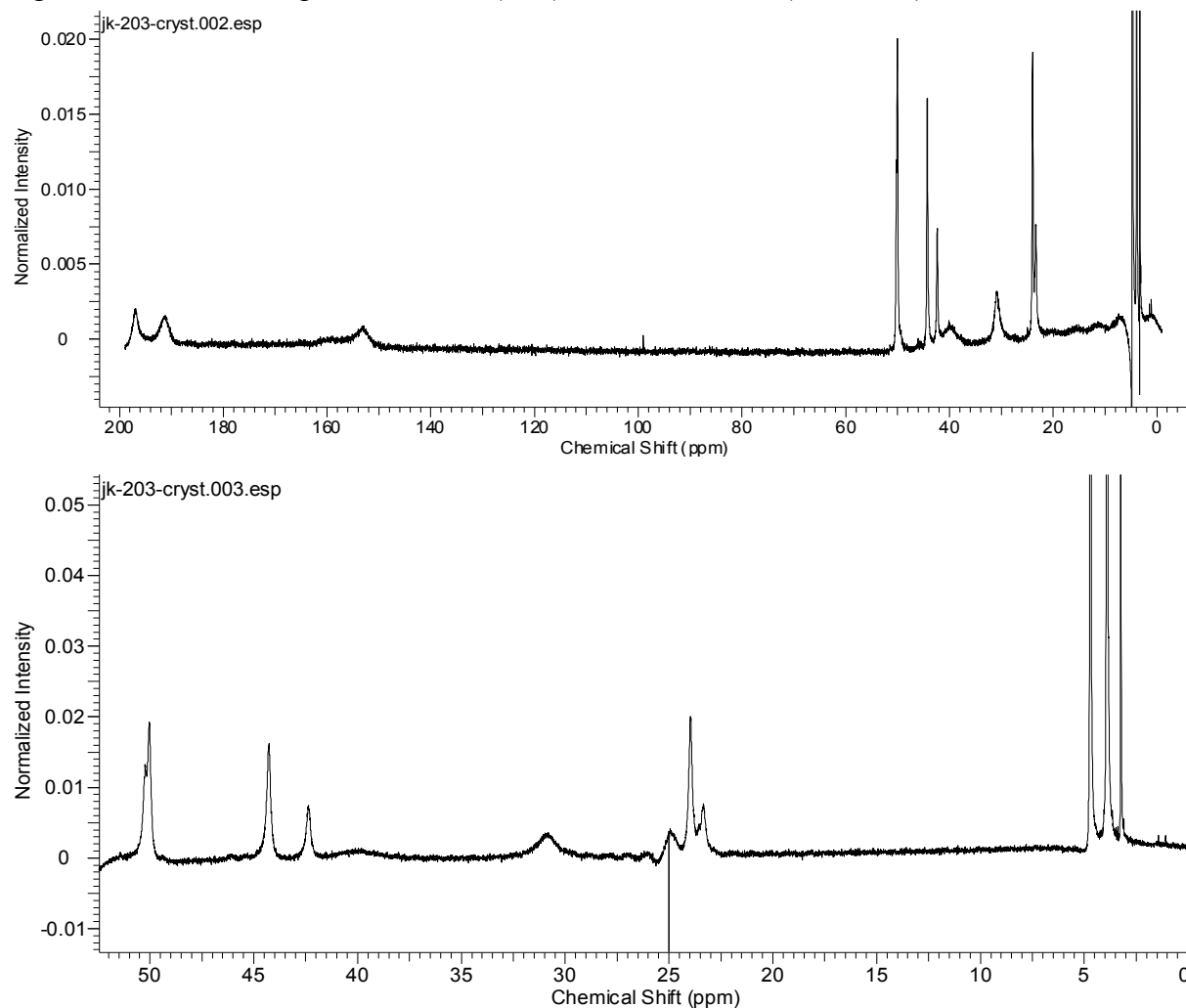


Figure S22: Magnetic moments of FeL4*SO₄ (Evans' method) at different temperatures

FeL4(SO₄) in aqueous solution

Temp. [K]	Magnetic Moment [BM]
298	4.96
303	4.97
310	4.98
323	5.00
333	5.00
343	5.00
353	4.98

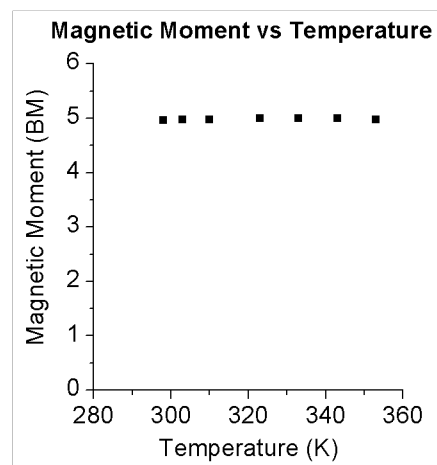
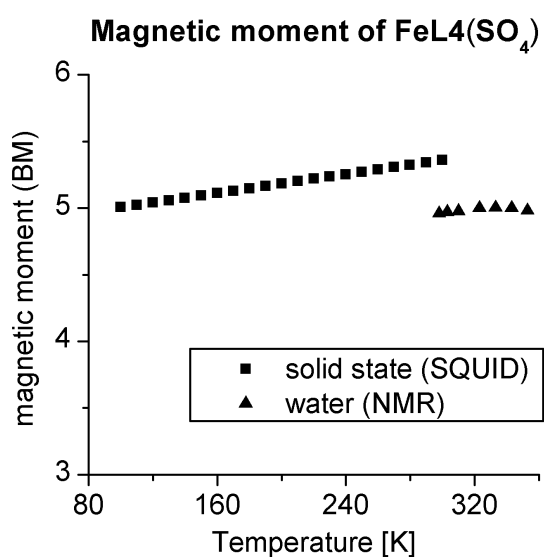


Figure S23: Temperature variation of magnetic moment of FeL4*SO₄ in the solid state (SQUID)



FeL4(CH₃CN) => ligand exchange leading to “intermediate” spin

Figure S24: ¹H NMR spectra in CD₃CN (298 K)

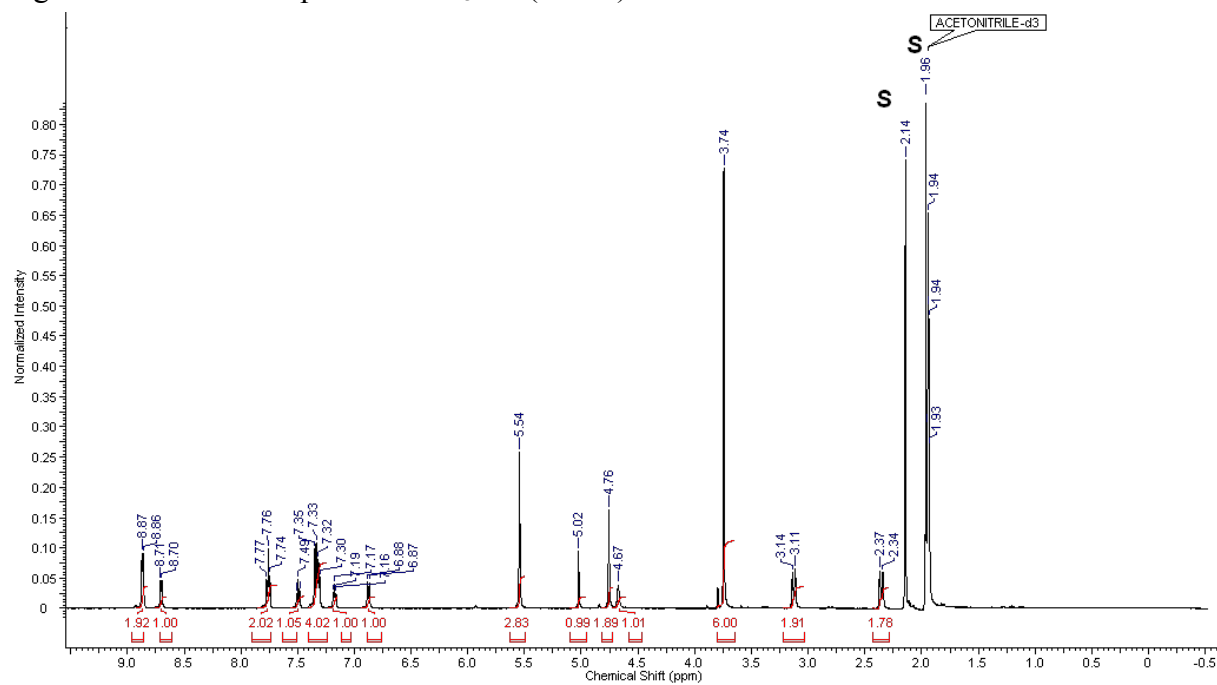


Figure S25: Variable temperature ¹H NMR spectra of FeL4*CH₃CN in CD₃CN (298 - 333 K)

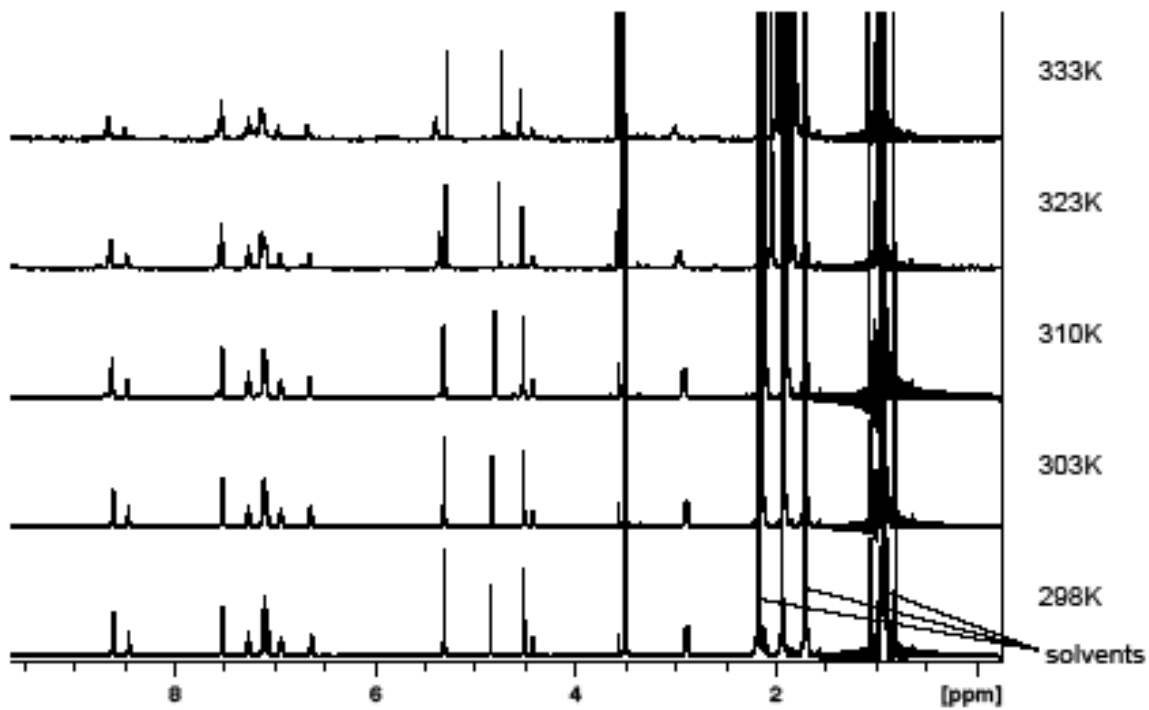


Figure S26: Variable temperature ^1H NMR spectra of FeL4*CH₃CN in Acetone-d6 (298 - 333 K)

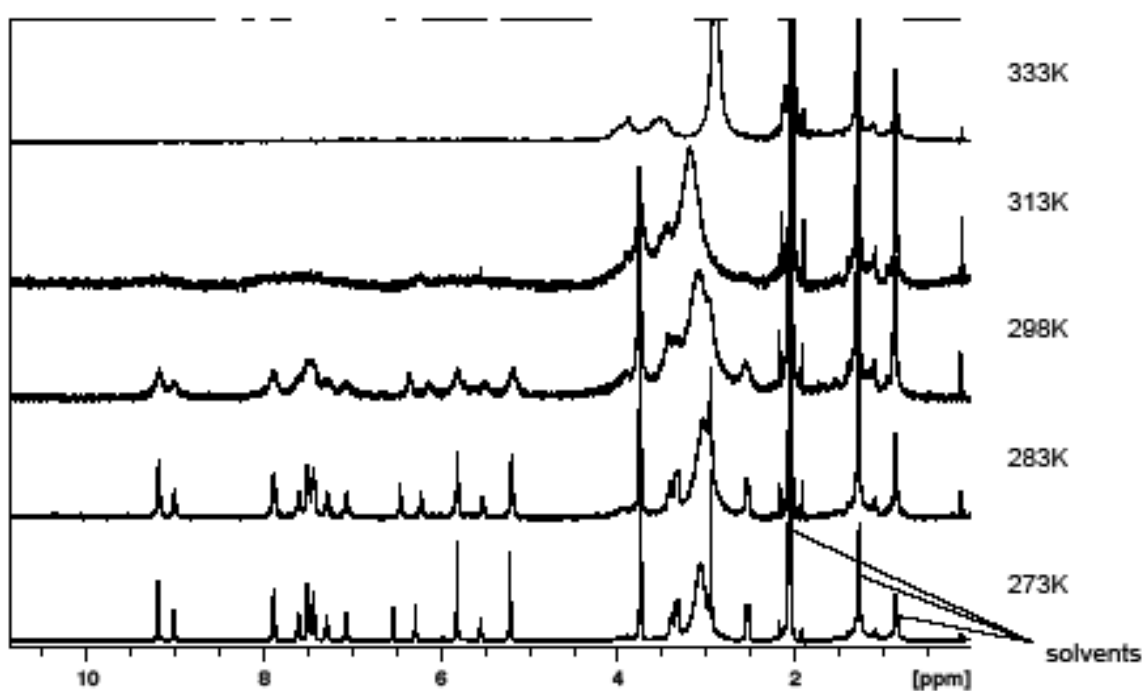
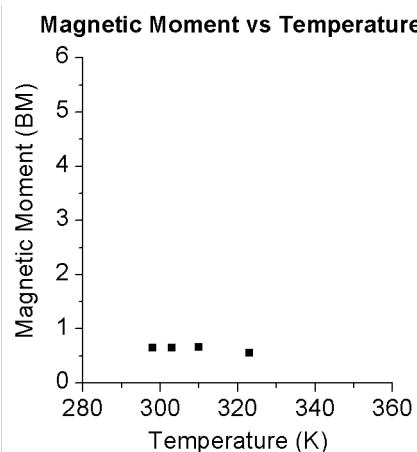


Figure S27: Magnetic moments of FeL4*CH₃CN (Evans' method) at different temperatures

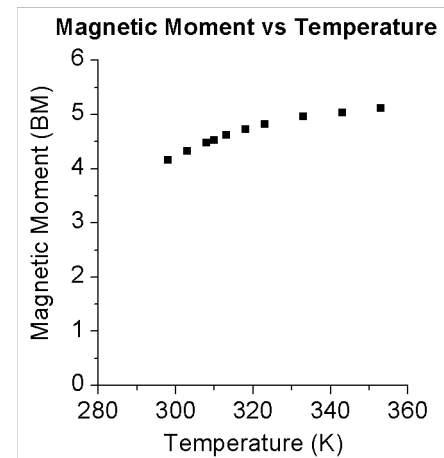
FeL4(CH₃CN) in acetonitrile-d3

Temp. [K]	Magnetic Moment [BM]
298	0,65
303	0,65
310	0,66
323	0,56



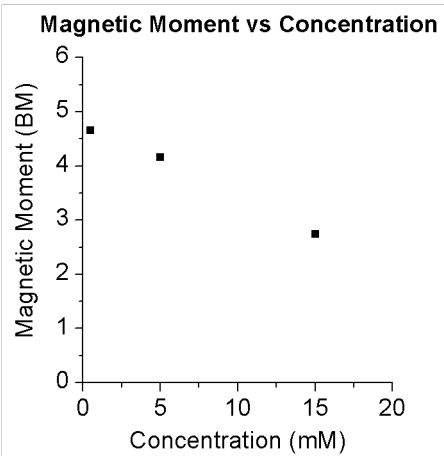
FeL4(CH₃CN) in aqueous solution

Temp. [K]	Magnetic Moment [BM]
298	4,16
303	4,33
308	4,48
310	4,53
313	4,62
318	4,73
323	4,83
333	4,96
343	5,03
353	5,12



**FeL4(CH₃CN) in aqueous solution
(298 K)**

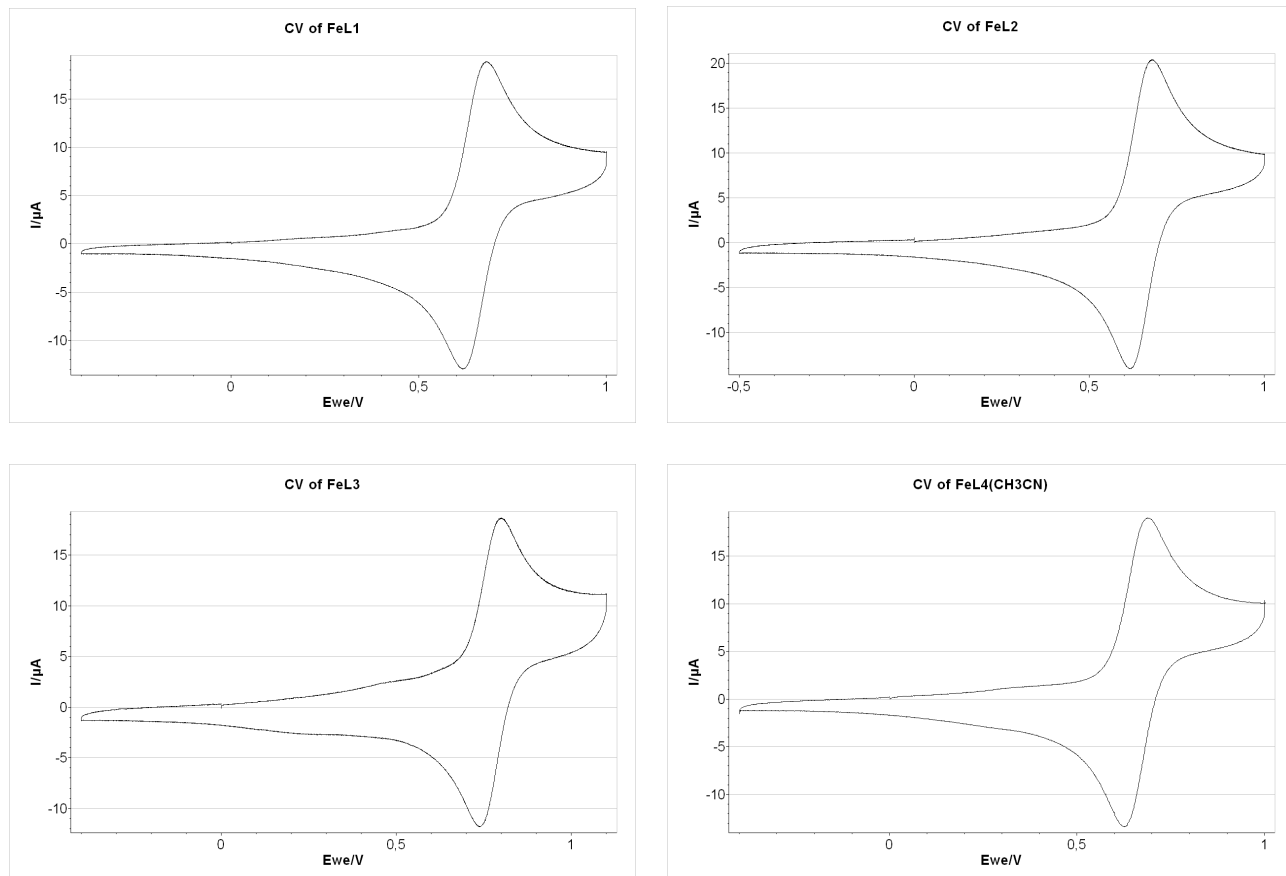
c [mM]	Magnetic Moment [BM]
0,5	4,66
5	4,16
15	2,74



Cyclic voltammetry:

Figure S28. Cyclic voltammograms of FeL1, FeL2, FeL3 and [FeL4(CH₃CN)] in acetonitrile.

Scan rate used during the experiments presented below was 100 mV/s but we have performed the whole series of experiments with a different scan rates (50, 150, 200 and 250 mV/s) proving the reversibility of the process.



References :

- [1] H. Borzel, P. Comba, K. S. Hagen, C. Katsichtis, H. Pritzkow, *Chem.--Eur. J.* **2000**, *6*, 914-919; R. Haller, U. Ashauer, *Arch. Pharm.* **1985**, *318*, 405-410.
- [2] M. G. N. Russell, R. W. Carling, J. R. Atack, F. A. Bromidge, S. M. Cook, P. Hunt, C. Isted, M. Lucas, R. M. McKernan, A. Hutchinson, K. W. Moore, R. Narquzian, A. J. Macaulay, D. Thomas, S.-A. Thompson, K. A. Wafford, J. L. Castro, *J. Med. Chem.* **2005**, *48*, 1367-1383.
- [3] D. F. Evans, *Journal of the Chemical Society (Resumed)* **1959**, 2003-2005; D. F. Evans, D. A. Jakubovic, *J. Chem. Soc., Dalton Trans.* **1988**, 2927-2933.
- [4] Konstantin P. Bryliakov, Eduard A. Duban, Evgenii P. Talsi, *Eur. J. Inorg. Chem.* **2005**, *2005*, 72-76.
- [5] F. Touti, P. Maurin, L. Canaple, O. Beuf, J. Hasserodt, *Inorg. Chem.* **2012**, *51*, 31-33.
- [6] D. H. Grant, *J. Chem. Educ.* **1995**, *72*, 39.
- [7] J. W. Turner, F. A. Schultz, *Inorg. Chem.* **2001**, *40*, 5296-5298.
- [8] D. Ostfeld, I. A. Cohen, *J. Chem. Educ.* **1972**, *49*, 829.
- [9] J. England, R. Gondhia, L. Bigorra-Lopez, A. R. Petersen, A. J. P. White, G. J. P. Britovsek, *Dalton Transactions* **2009**, 5319-5334.
- [10] L. L. Martin, K. S. Hagen, A. Hauser, R. L. Martin, A. M. Sargeson, *J. Chem. Soc., Chem. Commun.* **1988**, 1313-1315; T. H. Crawford, J. Swanson, *J. Chem. Educ.* **1971**, *48*, 382.
- [11] L. L. Martin, R. L. Martin, A. M. Sargeson, *Polyhedron* **1994**, *13*, 1969-1980.
- [12] B. Weber, F. A. Walker, *Inorg. Chem.* **2007**, *46*, 6794-6803.
- [13] J. L. Deutsch, S. M. Poling, *J. Chem. Educ.* **1969**, *46*, 167.
- [14] A. M. Brown, *Computer methods and programs in biomedicine* **2001**, *65*, 191-200.
- [15] D. C. Harris, *J. Chem. Educ.* **1998**, *75*, 119.